TU Delft

Delft University of Technology

Document Version
Final published version

Licence
CC BY

Citation (APA)
van Starrenburg, C., Mancheño, A. G., van de Koppel, J., van der Wal, D., Slegt, M. H., Schrama, M. J. J., Berg, M. P., van Wesenbeeck, B. K., Kalloe, S. A., Hofland, B., & Bouma, T. J. (2026). A trade-off approach to optimize nature-based flood defense designs: riparian willow forests as case study. *Ecological Engineering*, *225*, Article 107886. https://doi.org/10.1016/j.ecoleng.2025.107886

Important note
To cite this publication, please use the final published version (if applicable).
Please check the document version above.

Copyright
In case the licence states “Dutch Copyright Act (Article 25fa)”, this publication was made available Green Open Access via the TU Delft Institutional Repository pursuant to Dutch Copyright Act (Article 25fa, the Taverne amendment). This provision does not affect copyright ownership.
Unless copyright is transferred by contract or statute, it remains with the copyright holder.

Sharing and reuse
Other than for strictly personal use, it is not permitted to download, forward or distribute the text or part of it, without the consent of the author(s) and/or copyright holder(s), unless the work is under an open content license such as Creative Commons.

Takedown policy
Please contact us and provide details if you believe this document breaches copyrights.
We will remove access to the work immediately and investigate your claim.

This work is downloaded from Delft University of Technology.

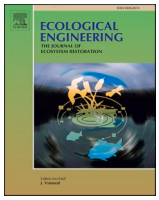
Ecological Engineering 225 (2026) 107886



Contents lists available at ScienceDirect

Ecological Engineering

journal homepage: www.elsevier.com/locate/ecoleng



A trade-off approach to optimize nature-based flood defense designs: riparian willow forests as case study

Corinne van Starrenburg [a,b,*], Alejandra Gijón Mancheño [c], Johan van de Koppel [a,d], Daphne van der Wal [a,e], Matthijs H. Slegt [f], Maarten J.J. Schrama [g], Matty P. Berg [h], Bregje K. van Wesenbeeck [c,i], Su A. Kalloe [c], Bas Hofland [c], Tjeerd J. Bouma [a,b]

[a] Department of Estuarine and Delta Systems, NIOZ Royal Netherlands Institute for Sea Research, P.O. Box 140, 4400 AC Yerseke, the Netherlands
[b] Faculty of Geosciences, Department of Physical Geography, Utrecht University, P.O. Box 80.115, 3508 TC Utrecht, the Netherlands
[c] Faculty of Civil Engineering & Geosciences, Delft University of Technology, Stevinweg 1, Delft 2600 GA, the Netherlands
[d] Groningen Institute for Evolutionary Life Sciences, University of Groningen, PO Box 72, 9700 AB Groningen, the Netherlands
[e] Faculty of Geo-Information Science and Earth Observation (ITC), University of Twente, PO Box 217, 7500 AE Enschede, the Netherlands
[f] Arcadis, P.O. Box 7895, 1008 AB Amsterdam, the Netherlands
[g] Faculty of Science, Institute of Environmental Sciences CML/Environmental Biology, Leiden University, 2333 CC Leiden, the Netherlands
[h] Amsterdam Institute for Life and Environment, section Ecology & Evolution, Vrije Universiteit Amsterdam, the Netherlands
[i] Deltares, P.O. Box 177, 2600 MH Delft, the Netherlands

ARTICLE INFO

Keywords:
Wave attenuation
Biodiversity
Ground-dwelling invertebrates
Salix
Floodplain forest
Forest structure
Hybrid solution

ABSTRACT

Nature-based solutions are increasingly recognized as effective and multifunctional components of climate-resilient flood protection. While tropical mangroves have received substantial attention, temperate riparian forests, particularly willow systems, offer comparable wave attenuation and biodiversity benefits, yet remain understudied. This study assesses the ecological and protective value of three types of willow floodplain forests: a so-called wild-grown willow forest, a pollard willow forest, and a willow plantation. Using field data from the Biesbosch National Park (the Netherlands), we quantified forest structure, ground-dwelling invertebrate diversity, and modelled wave attenuation under storm scenarios. Structural complexity and biodiversity were highest in the wild-grown forest, with significantly greater invertebrate order richness, larger body sizes, and more heterogeneous canopy architecture. The pollard forest showed the highest wave attenuation efficiency due to their dense, low-lying crown structures. The plantation forest showed lower values across both axes. We integrated these findings into a trade-off model evaluating ecological value, flood protection efficiency, and a 50-year simple cost analysis of each forest type as a hybrid solution alongside traditional dikes. While the pollard forest is the most spatially efficient for flood attenuation, the wild-grown system provides greater ecological value at lower lifecycle cost. Our results underscore the importance of tailoring hybrid flood defense strategies to local priorities - balancing biodiversity, spatial constraints, and economic feasibility. The framework developed here can inform ecosystem-based design in delta regions worldwide, supporting integrated climate adaptation that aligns safety with ecological resilience.

1. Introduction

Engineered flood defenses have protected low-lying, often densely populated areas for centuries, both from sea and river flooding (Zhu et al., 2020). These hard structures are often designed to reduce wave impacts (e.g., breakwaters), to enhance accretion (e.g., groynes) or to function as impermeable barriers against flooding (e.g., embankments and seawalls) (for overview see Schoonees et al., 2019). However, given

* Corresponding author at: Department of Estuarine and Delta Systems, NIOZ Royal Netherlands Institute for Sea Research, P.O. Box 140, 4400 AC Yerseke, the Netherlands.

E-mail addresses: corinne.van.starrenburg@nioz.nl (C. van Starrenburg), A.GijonMancheno-1@tudelft.nl (A.G. Mancheño), johan.van.de.koppel@nioz.nl (J. van de Koppel), daphne.van.der.wal@nioz.nl (D. van der Wal), matthijs.slegt@arcadis.com (M.H. Slegt), m.j.j.schrama@cml.leidenuniv.nl (M.J.J. Schrama), m.p.berg@vu.nl (M.P. Berg), B.K.vanWesenbeeck@tudelft.nl (B.K. van Wesenbeeck), S.A.Kalloe@tudelft.nl (S.A. Kalloe), B.Hofland@tudelft.nl (B. Hofland), tjeerd.bouma@nioz.nl (T.J. Bouma).

https://doi.org/10.1016/j.ecoleng.2025.107886
Received 12 August 2025; Received in revised form 23 November 2025; Accepted 21 December 2025
Available online 5 January 2026
0925-8574/© 2025 The Authors. Published by Elsevier B.V. This is an open access article under the CC BY license (http://creativecommons.org/licenses/by/4.0/).

a future with climate change and accelerating sea level rise, there is urgent need for climate-resilient cost-effective flood safety solutions to be implemented in the coming decades (Mcgranahan et al., 2007; Temmerman et al., 2013). This need causes nature-based solutions to gain lots of attention for either fully replacing or to support traditional engineered defenses by using so-called hybrid solutions (Saleh and Weinstein, 2016; Schoonees et al., 2019; Zhu et al., 2020). Vegetated foreshores can play a crucial role in hybrid flood defenses. They can dissipate wave energy before it reaches the flood defense so that this traditional structure can be less strong (e.g. Möller et al., 2014; Vuik et al., 2016; Zhu et al., 2020) and for instance a grass slope might suffice instead of a rock revetment (Kalloe, 2025).

Foreshores vegetated by woody mangrove forests are relatively well-studied as nature-based hybrid flood defense (e.g. Bao, 2011; Gijsman et al., 2021; van Hespen et al., 2021). Studies, both simulation and in situ, show that forest width is a major factor in protecting its hinterland from waves (Bao, 2011; Hashim et al., 2013; Hu et al., 2025; van Wesenbeeck et al., 2025; Zhou et al., 2022). Van Wesenbeeck et al. (2025) executed 216,000 model runs based on realistic global mangrove and wave characteristics and found that forests that are more than 500 m wide have considerable wave reduction that mostly exceeds 70 %. Below widths of 500 m, the exact wave reduction rates can vary between 10 and 90 % depending on the forest condition and structure, characterized by vegetation parameters such as tree density, tree size, and canopy closure (e.g. Bao, 2011; Hashim et al., 2013; van Wesenbeeck et al., 2025; Zhou et al., 2022). Mangroves do not only reduce incoming wave heights, but also attenuate currents and enhance sediment deposition, the latter causes that tidal-floodings result in a raising ground elevation which may enable compensating (partly or fully) for relative sea level rise (Beselly et al., 2023; Gijsman et al., 2024). Overall, mangroves shelter coastal communities from extreme events, reducing the estimated flood damages worldwide at a staggering 65 billion USD per year (Menéndez et al., 2020). For example, avoided embankment repair costs due to the presence of mangroves were estimated to range between 80,000–295,000 USD at selected sites in Vietnam (IFRC, 2012).

While mangroves are well known examples of woody vegetated foreshores, they only grow in tropical and subtropical regions (Lugo and Snedaker, 1974). In temperate zones, floodplain forests - often dominated by willow (*Salix* spp.) and alder (*Alnus* spp.) - serve a similar function in protecting embankments (e.g. Fang et al., 1999) and inland areas from flood impacts (Markus-Michalczyk and Michalczyk, 2023). These forests occur along rivers and estuarine zones with periodic salt exposure and have been shown to effectively reduce wave energy, stabilize soils, and trap sediments (Markus-Michalczyk and Michalczyk, 2023; Temmerman et al., 2013; Västilä and Järvelä, 2018). As such, they represent a key component of nature-based flood defense in lowland, riverine, and deltaic landscapes. It is less recognized that in temperate zones, such riparian forests perform comparable flood safety functions to those of mangroves, although recent evidence supports this notion. For example, in a true-scale flume experiments with mature willow trees, it was shown that they have wave damping rates of 5–25 % under extreme surge conditions for a forest as little as 40 m wide (van Wesenbeeck et al., 2022). Non surprisingly the wave reduction was greatest at water levels where trees occupied the largest area and stiffer branches around the water line, while damping rates decreased at high water levels. This reduction at higher water levels is because as storm conditions caused tree-branches to bend and allowed more of the wave energy to pass unobstructed on one hand and the area reduces as the branches are thinner and flexible on the other hand. So a strong and dense canopy attenuates better than the thin outer ends of the branches, which lay at higher heights. The forest structure at the level of the waves thus plays a crucial role in determining its wave-attenuating capacity (Kalloe et al., 2022; Mazda et al., 2006; Möller et al., 2014). By attenuating waves, willows can reduce the design requirements for the outer slope of embankments, thereby significantly reducing the flood-defense costs, while they have a relatively smaller effect on the dike height (Kalloe, 2025).

In densely populated estuaries and delta's, there is typically a high demand for limited space, imposing strong pressures on nature through habitat fragmentation by land conversions and pollutants related to intensive land-use (van Wesenbeeck et al., 2014; Zhai et al., 2019). So, besides a need to maintain flood-safety, there is also a need to improve environmental conditions both from an ecological and environmental regulations standpoint (European Commission, 2011; Sanders et al., 2019; van Wesenbeeck et al., 2014). The implementation of nature-based and hybrid solutions may thus offer multiple benefits by enhancing both flood safety while supporting biodiversity targets. Wetlands like mangroves and riparian forests are known to be biodiversity hotspots that offer unique habitats to flora and fauna (Pollen et al., 2013). In general, forest structure plays a crucial role in determining its ecological value (Ehbrecht et al., 2021). Structural heterogeneity influences species richness by increasing both habitat variability and resource distribution (Heidrich et al., 2023) and can outperform other variables in predicting species richness (Hekkala et al., 2023). Quantifying this complex forest structure is thus essential when assessing the value of floodplain and riparian forests both in terms of biodiversity as well as for wave attenuation.

While the implementation of riparian forests as nature-based hybrid solution will enhance both flood safety and biodiversity by offering structural heterogeneity, it is not clear whether the structural characteristics that promote flood resilience are equally effective in supporting biodiversity and vice versa. For example, riparian willow forests can have different forms: wild-grown (originally planted, but unmanaged) willow forests, willow plantations, and pollard willows (Rotherham, 2022).

A wild-grown forest is a naturally regenerating riparian forest that develops spontaneously in riverine areas, often dominated by species such as *Salix alba*, *Salix fragilis* and *Salix viminalis* (Markus-Michalczyk and Hanelt, 2019). There is no active human management, and their dynamic conditions support biodiversity and vital ecosystem services like sediment trapping and flood buffering (Peters et al., 2021). In this study, we refer to the term “wild-grown” to describe willow stands that, although originally planted, have been left unmanaged and have therefore developed natural growth forms and structural features—such as irregular crowns, fallen trees, and spontaneous regeneration—comparable to those found in naturally established forests (Franklin et al., 2002). This structural change usually occurs after pollard willows have been left unmanaged for minimal 10 years (Schepers, 1989). Therefore, even formerly planted forests, such as the Keizersdijk reserve in the Netherlands, unmanaged for 80 years, can be considered wild-grown, as the trees exhibit natural forms and growth patterns (Bijlsma et al., 2009). A pollard willow forest is a type of plantation. It consists of willows that are regularly pruned at a fixed height, usually 1.5–2 m above ground, or 1 m in plantations, encouraging the formation of thick crowns of shoots. These pollard willows historically served practical purposes, such as providing wood for basket weaving, fodder, fencing, or firewood (Rijksdienst voor het Cultureel Erfgoed (RCE), 2025; Stanton et al., 2014). In contrast, a willow plantation is a densely planted area of willows, typically managed for the periodic harvest of willow shoots used in traditional crafts and bioenergy. These plantations, often referred to as short-rotation coppice (SRC) in forestry and biomass productions, are usually commercial and differ from the pollard willow forests with shoots growing directly from the stems that are coppiced mainly mechanically at ground level (5–10 cm stem height) (DEFRA, 2004; Aylott et al., 2008).

While the two more controlled and actively managed growth forms (pollarded and plantation willow forests) offer the opportunity to have maximum frontal-area of branches (and biomass) in the wave-zone to maximize wave attenuation (van Wesenbeeck et al., 2022), a more natural forest type may offer the largest diversity in habitats thereby maximizing biodiversity (Heidrich et al., 2023; Tews et al., 2004). This study aims to develop a trade-off model towards optimizing biodiversity

while providing the required flood protection for three types of willow forests: a wild-grown willow forest, a willow plantation and a pollard willow forest (hereafter wild-grown forest, plantation and pollard forest, respectively).

The trade-off model is fed by a combination of *i)* in situ measurements on biodiversity proxies, *ii)* data-fed modelling on wave attenuation and *iii)* literature data for a costs. *Firstly*, ecosystem value and biodiversity of the different types of willow forests were estimated by measuring invertebrate diversity together with forest complexity parameters as proxy for the biodiversity potential. *Secondly*, the wave attenuation potential of the different types of willow forests was determined by modelling, using forest structure, including density, canopy size and height and tree frontal area, using wave height reduction as a proxy. We also considered boundary conditions such as wave height, elevation, tidal range, and inundation potential. *Thirdly* and finally, we performed a simple, comparative cost analysis for a hybrid solution with each of the forest types, compared to a traditional engineered dike. For this we included aspects like investment costs for land acquisition, maintenance expenses that include forest maintenance in case of hybrid solutions, and costs for upgrading revetments. It is noted that we did not translate the ecological value of nature as a monetary value given its temporal and spatially variable as influenced by context-dependency and methodologies (Schägner et al., 2013). To respect the multifaceted benefits of ecosystems without reducing them to economic terms alone, we separated the financial aspects of flood protection from ecological considerations. For this reason, we used the cost comparison within our trade-off analysis only to determine whether additional future investments could be used to achieve a higher biodiversity value of the nature-based solution rather than focus on safety alone.

2. Materials and methods

2.1. Study area

The Biesbosch National Park, encompassing approximately 9000 ha in the Netherlands (Fig. 1) is the world's largest freshwater tidal system and contains the country's largest willow forests. Highly anthropogenically influenced, it lies near densely populated areas and delivers key ecosystem services (Barendregt and Swarth, 2013). It is partially protected under EU environmental directives. Historically managed for willow twig production in the 18th - 19th centuries, the area has since reverted to a predominantly natural state, supporting diverse flora and fauna, including rare mosses, marsh marigold, owls, marsh birds, beavers, and various insects (Bijlsma et al., 2009).

This tidal freshwater wetland, influenced by micro- and meso-tidal regimes, arises from the interaction of nontidal freshwater riverine systems with intertidal estuarine wetlands. Its flooding dynamics and willow habitats support biodiversity and offer recreational value (Swarth et al., 2013). While some stands are pollarded, the majority is wild-grown. One willow plantation can be found, specifically planted to protect a dike from flooding. Our study focused on areas minimally disturbed by humans, suitable for scientific research.

2.1.1. Willow plantation

The studied plantation comprises five dense willow rows (13.5–15 m wide), separated by 3 m grass corridors, spanning approximately 500 m (three sections: 75 m, 250 m, 175 m). Willows are coppiced every two years at the ground, yielding stems of maximal 10 cm diameter (Fig. 2a). No other tree species are present; the understory is sparse. Three 5 × 5 m plots were randomly selected across rows to measure invertebrate diversity (Fig. 2b). Smaller plots (vs. 10 × 10 m) ensured: i) adequate spacing between traps, ii) distance from grass corridors to avoid disturbance, and iii) appropriate scale for the forest's high structural homogeneity.

2.1.2. Pollard willow forest

The pollard forest study site is situated along the Moldiep tidal creek in the Hollandse Biesbosch. This triangular-shaped forest consists of pollarded willows in rows with artificial creeks (Fig. 2c). Trees are coppiced every 3–4 years, and reed beds dominate the understory. The forest is subjected to approximately one meter tidal range. Three plots of 10 × 10 m were randomly selected, each at least 20 m apart (Fig. 2d),



Fig. 1. Map of the national park "de Biesbosch", a vast freshwater tidal wetland in the Netherlands, used as case study in this research. Source: Google Earth and Google Maps.

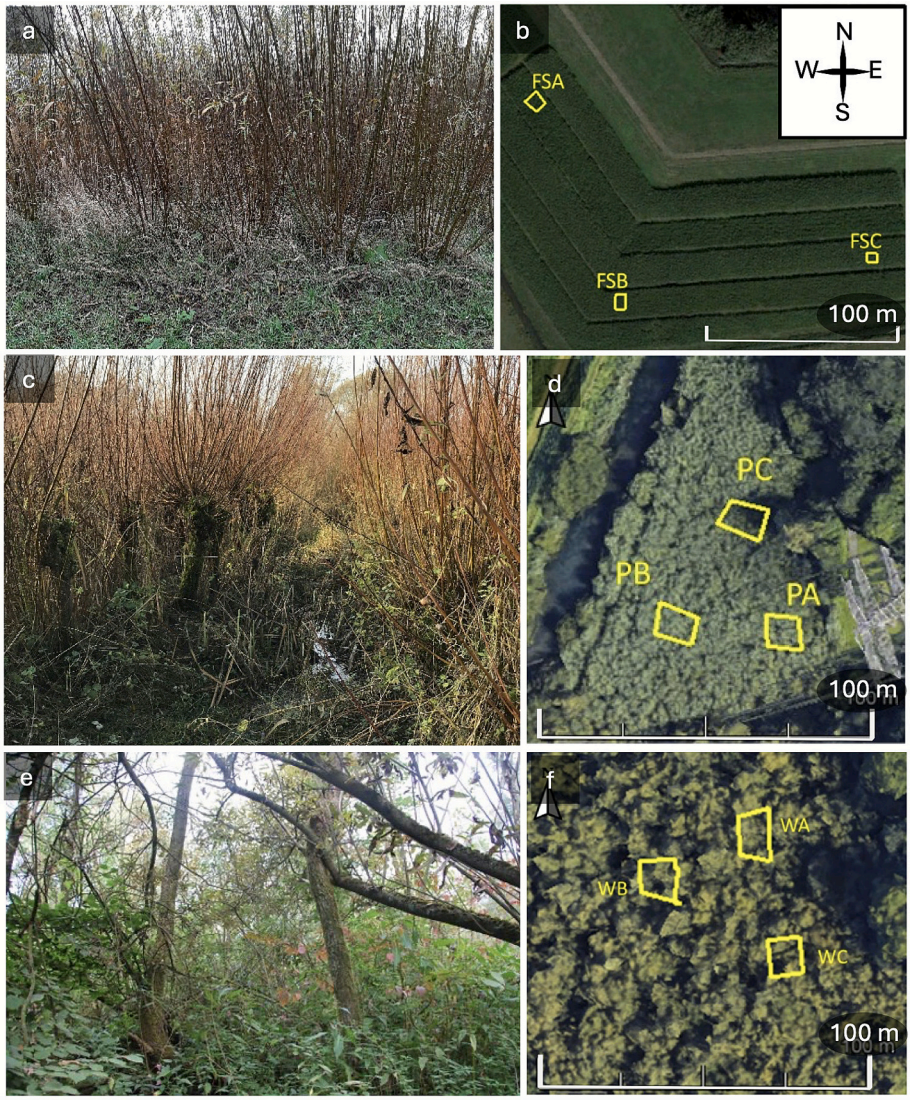


Fig. 2. Study location of three forests with a) plantation with particular shaped coppiced willows and b) the location of sampling in the plantation; c) pollard forest with trees in row, separated by creek and d) the plots distributed in the pollard forest; e) trees growing randomly with heterogeneous understory in the wild-grown forest and f) the plots distributed in the wild-grown forest.

subdivided into four 5 × 5 m subsections, due to dense reed cover, limiting access and visibility.

2.1.3. *Wild-grown willow forest*

Adjacent to the pollard forest, lays the "wild-grown" forest consisting of larger, unmanaged trees with fallen logs and a complex, less accessible environment (Fig. 2e). The understory, dominated by blackberry and nettles, contains various plant species. Like at the pollard forest, tidal fluctuations are about one meter. Three randomly chosen 10 × 10 m plots, at least 20 m apart, were used for the study (Fig. 2f).

2.2. *Forest structure parameters as indicators of habitat complexity and input to wave attenuation modelling*

Forest structure parameters were measured in situ as a proxy for habitat complexity and biodiversity potential, with greater structural heterogeneity typically supporting higher species richness (Tews et al., 2004; Heidrich et al., 2023). Moreover, structural attributes like canopy height, stem density, stem diameter, and most importantly the total branch frontal area, i.e. number and diameter of the branches are essential inputs for wave attenuation modelling, as they determine vegetation drag and energy dissipation (Kalloe et al., 2022; Möller et al., 2014; van Wesenbeeck et al., 2022).

2.2.1. *In situ assessment of forest structure and habitat characteristics*

Forest density was measured for the three selected plots per forest type, counting the number of trees to determine the number of trees per square meter. Additionally, the number of branches per tree was recorded for the plantation due to the unique tree shape characteristics. The Diameter at Breast Height (DBH; 1.3 m), was measured when possible. Due to the shape of the pollarded trees and those in the plantation, the D30 (diameter at 30 cm above ground) was measured for all trees (linear relationship with DBH by factor 1.2; $R^2 = 0.86$). Tree height was assessed per plot. In the pollard forest and plantation, both homogeneous regarding the tree shape, trunk height and branch length of five to ten trees were measured to derive the canopy height. No direct measurements of the canopy height were done in the wild-grown forest due to the great canopy height and limited accessibility of reaching the end of the branches. The litter layer thickness was measured by hand in autumn 2020, three times per plot per forest type. Dead wood was quantified by noting the number of fallen and standing dead trees per plot.

2.2.2. Digital elevation model of tree canopy height structure

We analyzed tree metrics and spatial forest heterogeneity using high-resolution digital elevation models (DEM) from the Dutch national elevation dataset (AHN), based on airborne laser altimetry, namely the digital terrain model (DTM) and digital surface model (DSM) (layer map 38DZ1: wild-grown and pollard forest; layer map 44BN2: plantation). All areas of interest were mapped in December 2019. The pollard forest and the plantation study plots were both coppiced in 2018. Layers were projected in the Amersfoort / RD New coordinate system (EPSG:28992). The Canopy Height Model (CHM) was calculated by subtracting the DTM from the DSM, showing tree canopy heights. Selected polygons encompassed the broader study area and precise plots. As surrounding forests revealed little differences from the plots (see Appendix A, Table A1 & Fig. A1), larger areas were used for analysis. A binary mask filtered out vegetation below 1 m (values $\geq$1 set to 1; <1 set to 0), isolating trees. Forest cover was calculated and multiplying the mask with CHM resulted in true tree heights, from which mean tree height and standard deviation (i.e. heterogeneity) were computed per polygon (Appendix A, Table A1).

2.3. Invertebrate biodiversity assessment as proxy for forest-biodiversity potential

We use biodiversity indices based on in situ invertebrate studies, combined with both in situ and remotely determined forest structure characteristics. Ground-dwelling invertebrates were targeted as biodiversity proxy across the three forest types.

2.3.1. Ground-dwelling invertebrates: sampling and diversity assessment

Ground-dwelling invertebrates were sampled using 36 enclosed pitfall traps across the three forest types from November 26 to December 14, 2020. The traps were active for 17 days, checked at 72-h intervals. A smaller campaign was conducted in summer 2022, used only indicative for order abundance and richness (Fig. 4). Traps were placed between trees and minimal 50 cm from creeks to minimize the risk of flooding. The pitfall traps consisted of two cups placed in the ground, level with the ground surface, and surrounded by a 50 × 50 cm-square of plexiglass enclosure. The enclosure allows sampling of all invertebrates within the area. Detailed trap construction and sampling procedure are described in Appendix A2, Fig. A2, the functioning of the trap can be seen in Appendix A2, Fig. A3.

Invertebrate specimens were classified to order level (e.g., *Aranea* for spiders) and abundance per m^2 as well as richness per forest type was determined (detailed description Appendix A3). The body size (length) of all individuals from four orders was measured, but further analysis focused on order of spiders (*Araneae*) and beetles (*Coleoptera*).

2.3.2. Calculating Diversity Indexes based on in situ invertebrate measurements

Both, abundance and richness were used to calculate a Diversity Index, based on the Simpson's Diversity Index 1- D, the most appropriate index for our study (Magurran, 2005). Note: Diversity index refers here to order-level richness and abundance, not species-level indices like Simpson's. Diversity Index D being defined as:

$$D = \frac{\Sigma\, n(n-1)}{\mathrm{N}(\mathrm{N}-1)} \quad (1)$$

Where:
n = number of individuals per order.
N = sum of all individuals.

2.3.3. Diversity metrics and statistical comparison across forest types

Alpha and beta diversity were calculated to assess invertebrate biodiversity across the three forest types. Alpha diversity was quantified as the number of invertebrate orders per trap and beta diversity using the Sørensen dissimilarity index:

$$\text{Sørensen Index} = 1 - \frac{2C}{A+B} \quad (2)$$

Where C is the number of shared orders between two traps, and A, B are the total number of orders in each trap. Sørensen dissimilarity was computed for each plot and forest type. Beta diversity was assessed at two scales: Intraplot (i.e., variation between traps within plots) and Interplot, (i.e., variation between plots within a forest type). **Kruskal–Wallis tests** were used to statistically compare biodiversity metrics between forest types.

2.4. Modelling wave attenuation by willow forest types as proxy for flood safety

Here wave height reduction (hereafter also denoted as wave attenuation) was used as a quantitative proxy for flood safety. Estimates were based on the approach of Gijón Mancheño et al. (2024), which calculates wave reduction through vegetated fields considering wave energy losses via two mechanisms: wave breaking (as waves become unstable when approaching shallow coastal areas) and wave energy dissipation by vegetation (due to the physical obstruction) as established by Mendez and Losada (2004). The wave dissipation term associated to vegetation resistance is integrated over the water column in 1-cm intervals, enabling detailed modelling of vertical variations in vegetation frontal surface area, similar to Suzuki et al. (2012) but with higher vertical resolution. This approach has been validated for wave attenuation by willows (van Wesenbeeck et al., 2022) and salt marshes (Vuik et al., 2016), as detailed in Gijón Mancheño et al. (2024).

The frontal area of trees (Appendix C, Fig. C1 & C2) was modelled based on stem and branch areas, excluding leaf area, as leaves are shed from the trees in the storm season when the flood safety function is required and since they were found to have nearly no effect on wave attenuation in real-scale flume experiments with willow trees (see Appendix 1 for the assumptions behind the frontal surface area model). Willow forests were simulated for the design water levels for flood protection as outlined by Kalloe (2025), which are summarized in Table 1.

So called return periods describe how often, on average, a storm of a certain intensity or larger is expected to occur (Gumbel, 1941). Return periods are widely used in flood defense design to set safety standards and simulate the expected stresses that structures like dikes or levees must withstand. These hydraulic conditions were determined by the probabilistic methods in the HYDRA-NL computational software, as used by the Dutch government (Duits, 2020). Model simulations commonly incorporate specific return period events (in this work: 1/10, 1/100, 1/1000, 1/10.000 and 1/100.000 year storms) to evaluate the performance of flood defenses under varying hydrodynamic stresses.

Drag coefficients (empirical factors that represent wave damping by aquatic vegetation) from real-scale wave flume experiments with willow trees were used (van Wesenbeeck et al., 2022). They provided values for the drag coefficient (Cd) as a function of the Keulegan-Carpenter number (KC), defined by:

Table 1
Design wave conditions and water levels at the selected willow forest sites from Kalloe (2025). Significant wave heights (Hs; m), peak periods (Tp; *sec*) and water depths (h; m) are provided for events with probabilities between 1/10 and 1/100000 years (Frequency).

	Plantation			Pollard & Wild-grown forest		
Frequency	Hs (m)	Tp (s)	h (m)	Hs (m)	Tp (s)	h (m)
1/10	0.40	1.69	2.80	0.53	2.08	2.51
1/100	0.71	2.61	3.26	0.70	2.30	2.92
1/1000	1.02	3.21	3.63	0.87	2.50	3.26
1/10.000	1.32	3.67	3.94	1.04	2.68	3.58
1/100.000	1.65	4.08	4.28	1.24	2.85	3.94

$$KC = \frac{u_w T_p}{b_{v,mean}}$$

where u_w is the depth-averaged peak horizontal orbital wave velocity calculated by linear wave theory, based on a significant wave height H_s, peak period T_p and water depth h; $b_{v,mean}$ is the mean diameter of the vegetation (stems and branches) averaged over the water depth and branch orders. As shown in Fig. 3, we parameterized the relationship between Cd and KC with a linear function up to the maximum Cd value, following Graham (1980), and applied a hyperbolic decay for very high KC values, as described by Gijón Mancheño et al. (2021) The calculation of the average diameter for different forest types is explained in Appendix C.

2.5. Combining wave attenuation and biodiversity value

To compare directly, we analyzed wave attenuation potential and biodiversity value on a spatial scale. Wave attenuation for the three forest types was modelled for forest widths of 50–500 m. Biodiversity was assessed using a species-area relationship (SAR) approach. This was achieved by: (1) calculating the average number of orders observed in the three subsamples per plot (0.25 m^2) for each forest type, (2) determining the average cumulative number of orders from all 10 m^2 plots per forest, and (3) calculating the cumulative number of orders per forest for an approximate forest width of 50 m, corresponding to a total area of 2500 m^2.

2.6. Cost estimation for willow forest-based flood defense strategies

Assigning monetary value to nature often underappreciates its intrinsic and functional significance. These values are highly context-dependent, temporal and spatially variable and influenced by methodologies (Schägner et al., 2013). A synthesis of economic values for 23 ecosystem services across 15 biomes (Brander et al., 2024) highlights significant variations in value magnitudes and data availability. While some biomes and services are well-represented, others lack sufficient data despite their potential value, so that total biome values are likely underestimated (Brander et al., 2024).

We conducted a highly simplified cost analysis comparing different dike-forest combinations to see whether future investments could improve natural value alongside safety. Land acquisition and 50-year maintenance costs per kilometer of dike were estimated based on literature and informal consultations with governmental officials. Forest widths required for safety resulted from our modelling.

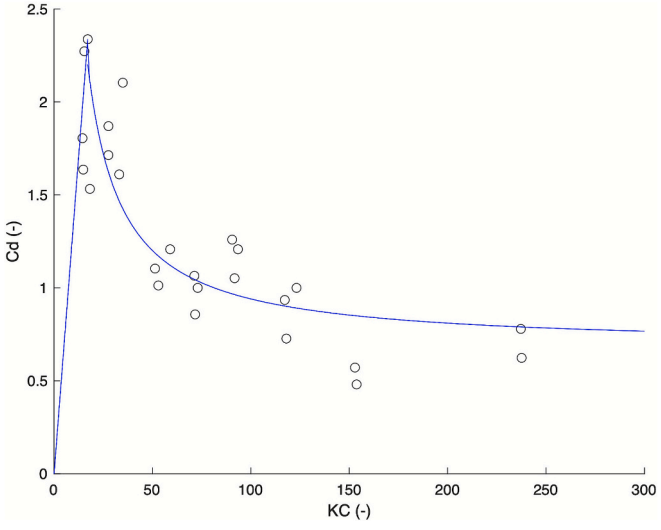


Fig. 3. Fit to drag coefficients measured by van Wesenbeeck et al. (2022), consisting of a linear function between KC = 0 and the relative maximum of Cd, and a hyperbolic decay to Cd = 0.5 towards infinite KC values.

We used:

$$C_{50} = A \times (L + P + M_{50}) \quad (3)$$

with:

C_{50}= costs for 50 years (€) of nature-based flood defense of a given stretch (*dw*)

L = average land price (€/ha)

M_{50} = maintenance costs in 50 years (€/ha)

P = planting costs specific forest (€/ha)

A = area (ha), calculated as:

$$A = \frac{w \times dw}{10^4} \quad (4)$$

with:

w = modelled width forest to meet wave attenuation requirement (m)

dw = stretch of coast, here 1 km (m)

The yearly maintenance costs M_1 (€/ha) are calculated as:

$$M_1 = y + \left(\left(\frac{x}{n}\right) \times P\right) + O \quad (5)$$

with:

y = average yearly costs (€/ha)

x = number of years of interest (years)

n = average number of years in between sub-sequent coppicing (years)

P = costs coppicing (€/ha)

O = other yearly costs (€/ha)

3. Results: structural, ecological and functional differences between willow forest types

3.1. In situ measurements of forest structure and invertebrate communities

The comparison of forest attributes across the three forest types revealed distinct ecological and structural differences. We measured 15 variables: six forest structure parameters and nine invertebrate-related variables (Fig. 4). Additionally, alpha diversity, interplot beta diversity and intraplot beta diversity were calculated for invertebrates, resulting in 18 parameters analyzed overall. Among these, the wild-grown forest exhibited the highest values for 12 parameters, indicating greater biodiversity potential. In Fig. 4 we show per forest system (plantation, pollard forest or wild-grown forest) the measured and calculated parameters with on top the ones relevant for the forest structure, followed by the invertebrate study.

3.1.1. Forest structure and habitat complexity

Structural characteristics of the three forest types showed significant variation (exact significance values in Appendix B, Table B1). The pollard forest exhibited statistically significant the largest average D30 (23.2 cm ± 14.7, $p < 0.001$). Canopy height was greatest in the wild-grown forest, averaging 10.5 m ± 5.7, while tree density was markedly lower (16 trees/10 m^2 ± 4) compared to the plantation (79 trees/10 m^2 ± 11) and the pollard forest (52 trees/10 m^2 ± 8). The wild-grown forest also had a significantly thicker litter layer (3.4 cm) than the plantation and pollard forest which had a similar thickness of litter layer (both 1.7 cm, $p < 0.01$; see supplementary Table B1.2 for exact values). Dead tree abundance varied among the forest types with statistically significant ($p < 0.05$) differences and the wild-grown forest having the highest number (6.7 trees/10 m^2), followed closely by the pollard forest (6 trees/10 m^2). However, in the pollard forest, dead stems remained upright, whereas in the wild-grown forest, they were mostly fallen over, increasing habitat heterogeneity. In contrast, the

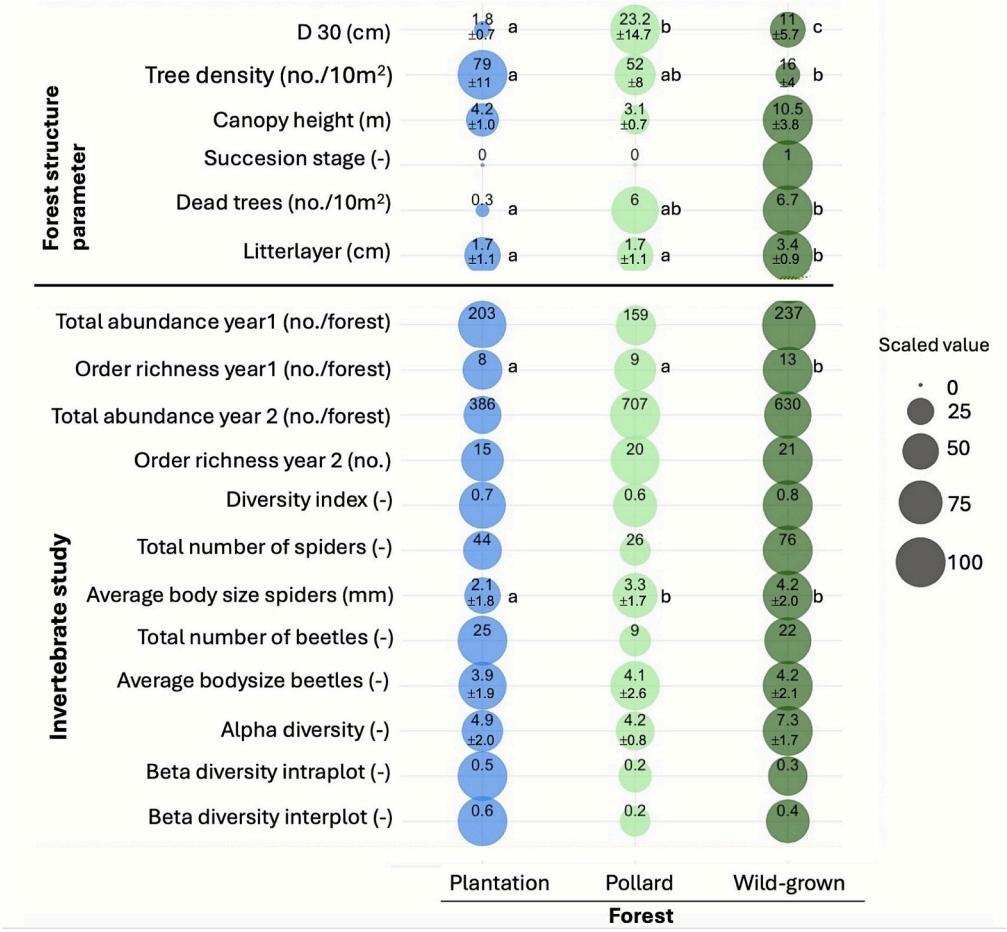


Fig. 4. Biodiversity and invertebrates parameters based on in situ measurements. Bubble sizes are scaled relative to the largest value within each parameter: the largest value is shown as 100 %, with the other two scaled proportionally. Actual values are shown in bubbles as well as standard deviation. Colors indicate forest type: blue = plantation, light green = pollard, dark green = wild-grown. Statistical differences between forest types were assessed using Kruskal–Wallis tests. Shared letters (a, b and c) denote no significant difference, while different letters indicate significant difference between groups (Dunn's posthoc test, $p < 0.05$). Overall, the wild-grown forest showed highest values compared to plantation and pollard, indicating greater biodiversity. (For interpretation of the references to colour in this figure legend, the reader is referred to the web version of this article.)

plantation had very few dead trees (0.3/10 m^2), showing lower structural complexity.

3.1.2. Ground-dwelling invertebrate study

The wild-grown forest supported the highest invertebrate abundance and order richness, the latter being significantly greater than in the other forest types ($p < 0.05$). The secondary (summer) sampling showed the highest invertebrate abundance in the pollard forest, but this was not further analyzed and is only presented as descriptive support. Spider densities were highest in the wild-grown forest, where individuals were also significantly larger compared to the plantation and pollard forest ($p < 0.05$). Beetle abundance peaked in the plantation, while beetles in the wild-grown forest were slightly larger. Although overall invertebrate abundance and beetle size differences were not statistically significant ($p > 0.05$), the wild-grown forest had the highest diversity index, suggesting a more complex invertebrate community. Overall, the wild-grown forest consistently supported more diverse and abundant invertebrate communities and larger predatory invertebrates, likely due to its greater habitat complexity, which included a thicker litter layer, higher dead tree abundance, and greater structural diversity.

The relationship between the thickness of the litter layer and ground-dwelling invertebrate abundance was found to be approximately linear across all forest types ($R^2 = 0.55$, Fig. 5A). This was weakest for the wild-grown forest ($R^2 = 0.56$) and strong for the pollard forest ($R^2 = 0.82$) and plantation ($R^2 = 0.83$). The relationship between litter layer and species order number (Fig. 5B) appeared strongly linear when analyzed using averaged data ($R^2 = 0.9$). However, when examining individual data points, no significant linear correlation was observed. This discrepancy suggests that the observed trend in the aggregated data may be influenced by the grouping process or averaging, potentially masking underlying variability or non-linear patterns.

3.1.3. Alpha and beta diversity of invertebrate communities

Alpha diversity values varied across traps, plots (Appendix B, Table B2), and forest types (Appendix B, Table B3). In the plantation forest, alpha diversity ranged from one to seven orders per trap, with the average per forest type at 4.9 ± 2.0 orders. For the pollard forest, alpha diversity ranged from three to five orders per trap, with the average per forest type at 4.2 ± 0.8 orders. The wild-grown forest showed the largest alpha diversity, ranging from four to nine orders per trap, with the average per forest type at 7.3 ± 1.7 orders. The Intraplot beta diversity was observed within the plots as 0.47 for the plantation, 0.15 for the pollard forest, and 0.32 for the wild-grown forest. The Interplot beta diversity was largest in the plantation (0.58), followed by the wild-grown forest (0.45), and pollard forest (0.2).

3.1.4. Variation in spider and beetle body size

Body size distribution of spiders and beetles varied significantly

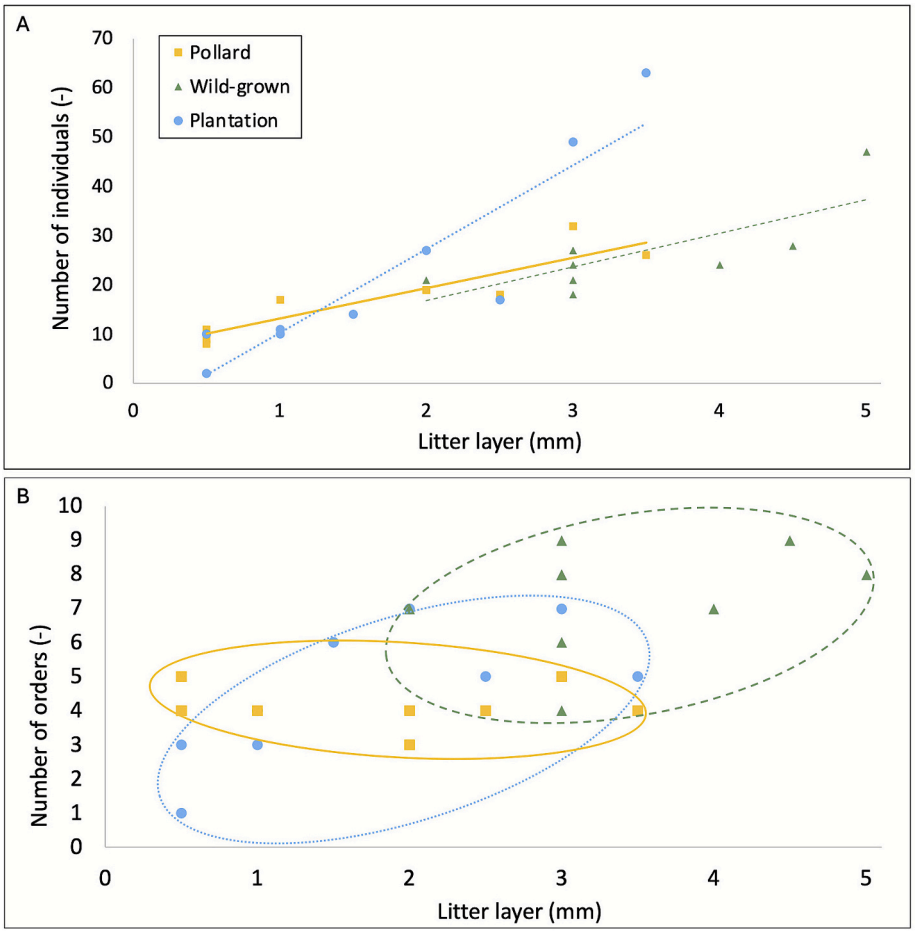


Fig. 5. Litter layer thickness and relationship with A) number of individuals that is positive and near-linear and B) number of orders found in situ for planation (dot), pollard forest (square) and wild-grown forest (triangle), showing a trend but no clear relationship.

among the three types of forests (Fig. 6). In the plantation, there was a pronounced peak in small-sized individuals for both spiders and beetles. Most spiders measured less than 2 mm, beetles were predominantly smaller than 4 mm. Only one to five larger individuals were recorded for either group, indicating a skewed size distribution favoring smaller organisms. In contrast, the pollard forest showed a slightly different pattern. Spiders were generally smaller, with sizes peaking below 2 mm and a maximum size of 8 mm. Beetles similarly had a small size range trend, with the majority being less than 4 mm, except one outlier measuring 10 mm.

The wild-grown forest exhibited a more even distribution of body sizes for both spiders and beetles. Spider individuals were predominantly 3–4 mm and 5–6 mm in size, but all size classes were represented except for the largest (>11 mm). Beetles in the wild-grown forest also showed a broader size distribution, with most individuals under 4 mm but several larger ones present. Five beetles measured 5–6 mm, and two individuals fell into the 9–10 mm category, indicating a greater variety of sizes compared to the plantation and pollard forest. Overall, these results suggest that the wild-grown forest supports a broader spectrum of body sizes for both spiders and beetles.

3.2. *Tree metrics derived from Digital Elevation Models*

Tree metric analyses revealed distinct differences in forest cover, tree height, and structural complexity among the three forests. Forest cover was highest in the wild-grown forest (60.1 %), whereas the pollard forest (32.6 %) and the plantation (29.8 %) had similar, considerably lower coverage (Fig. 7, see also Appendix A1, Table A1).

Tree height varied substantially across forest types. The plantation and pollard forest exhibited similar overall structures, with average canopy heights of 1.6 m (± 0.5 m) and maximum tree height of 4.2 m and 4.1 m in plantation and pollard forest, respectively. Within the smaller study plots specifically, average heights were slightly lower: 3.1 m for the plantation and 2.8 m for the pollard forest. In contrast, the wild-grown forest displayed a significantly greater average canopy height of 3.9 m, a maximum height of 16.9 m (± 2.4 m), indicative of a more heterogeneous and mature forest structure. Within the study plots of the wild-grown forest, the maximum tree height reached 12.5 m, while mean and standard deviation values were consistent with those observed across the broader forest area. Tree height data were not log-transformed, as values were derived from canopy height models (CHM) in QGIS using Sentinel data, which represent aggregated remote sensing outputs. Retaining raw values allows for clear structural comparisons in meters across forest types.

While the plantation and pollard forest had comparable tree coverage (~30 %) and relatively homogeneous structures, the wild forest exhibited greater canopy height, higher structural variability, and increased dead tree abundance. Thus, remote sensing analyses confirmed tour in situ findings that the wild-grown forest is the most structural heterogeneous system in our study. The agreement between in situ measurements and remote sensing data highlights the influence of forest management on canopy complexity and habitat heterogeneity.

3.3. *Wave attenuation performance of different forest types*

For all forest widths and storm return periods, pollarded trees

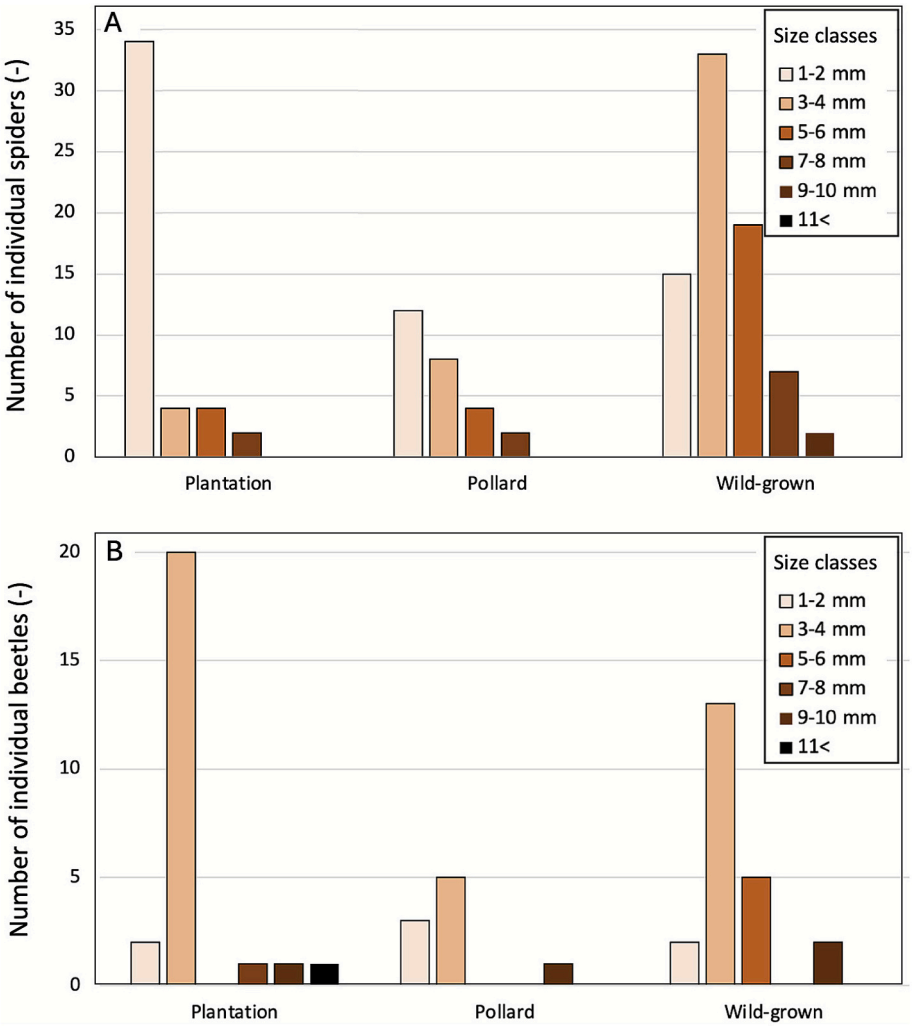


Fig. 6. Size distribution for predator ground-dwelling invertebrates for plantation, pollard forest and wild-grown forest with number of individuals per size category ranging from 1 to 2 mm to >11 mm with A: spiders, and B: beetles. A balanced size-category distribution is generally associated with structural complex habitats and good ecological conditions.

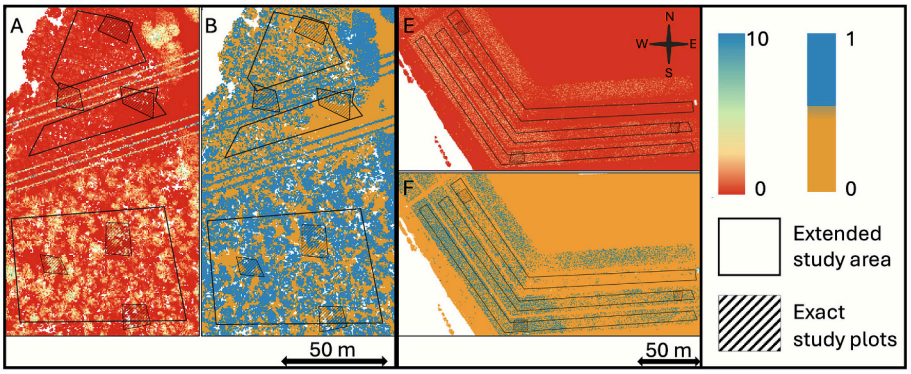


Fig. 7. A) forest cover as continuous canopy height layer of the vegetation displayed, after applying a threshold of 1 m and B) binary image, showing in orange, vegetation <1 m and in blue all areas with vegetation higher than 1 m. On the top are polygons of the pollard forest (two larger ones and three smaller) and the lower polygons containing the area of the wild-grown forest (one large containing the three exact plots); C) and D) show the same for the plantation. (For interpretation of the references to colour in this figure legend, the reader is referred to the web version of this article.)

demonstrated the greatest wave reduction rates (Fig. 8b) due to their large submerged frontal area (see Fig. C2, Appendix C1). Their submerged area was largest for the water levels and wave heights associated with a 10-year return period. However, as water levels rise with longer return periods, a smaller proportion of the water column was obstructed by pollarded trees at elevations with lower orbital velocities, resulting in reduced resistance to waves and thus increased wave transmission (Fig. 8b).

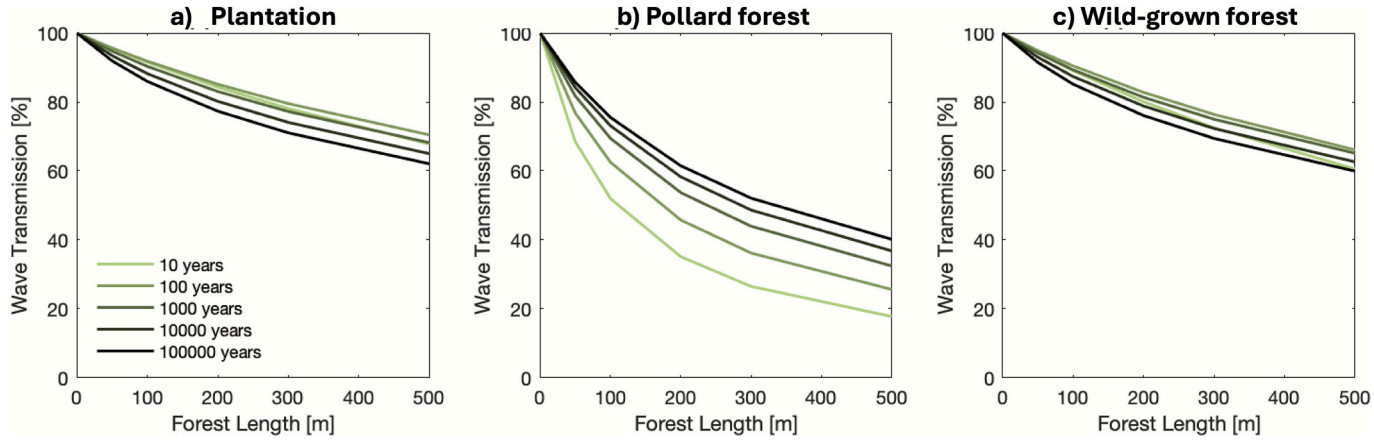


Fig. 8. Wave transmission through the different forest types as a function of forest width for return periods between 10 and 100,000 years for (a) plantation, (b) pollard forest, and (c) wild-grown willow forest.

In comparison, plantation (Fig. 8a) and wild-grown forest (Fig. 8c) exhibited comparable rates of wave reduction, both were generally less effective than pollarded trees. Both the plantation and wild-grown forest had comparable overall surface areas (Appendix C, Fig. C1 & C2), but the wild-grown forest featured a larger submerged area near the ground due to fallen mother trees and a smaller surface area distributed over a greater tree height at higher elevations. These structural differences created variations in wave attenuation, particularly at lower water levels and wave heights. Under extreme conditions (storms with return periods between 10,000 and 100,000 years), the performance of plantation and wild-grown forest became comparable. Flexibility differences among the three forest types had a small impact on wave attenuation outcomes (see Appendix C, Fig. C3). Interestingly, the pollard forest performed best under high return periods and the other two performed worst. This is likely due to differences in biomass distribution over the vertical.

Overall, comparisons across different forest types and widths emphasized the critical role of forest width: narrow forests of 50–150 m led to wave transmission rates of 85–95 % for plantation and wild-grown forest, and approximately 60–80 % for the pollard forest (for the highest return periods, Fig. 8). In contrast, a 500 m forest width significantly lowered wave transmission to 60–70 % for plantation and wild-grown forest, and to around 20–40 % for the pollard forest.

3.4. *Trade-off between biodiversity gains and wave attenuation efficiency*

Our findings revealed a strong relationship between forest structure and wave attenuation, with the pollard forest demonstrating the greatest reduction in wave transmission and both wild-grown forest and plantation showed similar wave reduction patterns (Fig. 9). Since a forest cannot physically be 0.1 or 10 m wide, these values were omitted in the figure for clarity (see Appendix C, Table C1 for full model results across log scale). A wave transmission of 100 % represents the absence of a vegetation effect. From this point onward, the model showed how wave transmission decreases with increasing vegetation width. The smallest area used for invertebrate richness reflected the actual sampling unit (0.25 m^2), allowing biodiversity patterns to be assessed from the finest observational scale upward. Plotting both datasets on a log scale highlighted trends across several orders of magnitude.

We exemplify this, using the simulated 10,000-year storm event for the three forests. At a 100 m forest width, the pollard forest attenuated 25 % of wave energy, while plantation and wild-grown forest achieved approximately 10 % attenuation. At 500 m, the pollard forest reduced waves to 40 % of their initial size, compared to 60 % for plantation and wild-grown forest. (see Appendix C, Table C1 for reductions of all storm scenarios). These results indicate that larger forest widths significantly

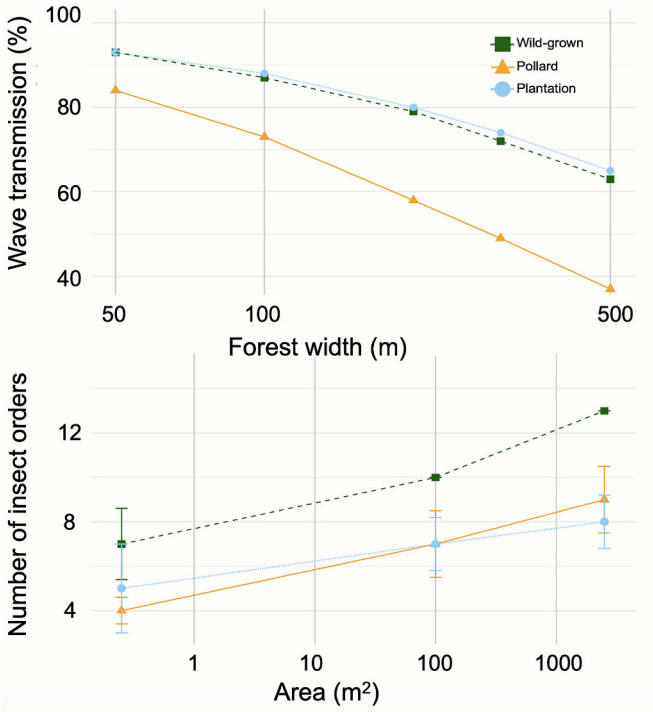


Fig. 9. Modelled wave transmission and determined number of invertebrate order (in situ) for each forest (wild-grown forest, pollard forest and plantation) as a function of forest width (m) and area (m^2).

enhanced wave attenuation across all forest types, with pollard forests proving particularly effective in reducing wave transmission. For safety requirements a reduction of 30–40 % is necessary, meaning that 150 m wide pollard forest or 500 m width of plantation and wild-grown forest would be required to attenuate sufficient wave energy in a nature-based solution.

In parallel, we observed a clear positive relationship between forest area and biodiversity, with the wild-grown forest consistently exhibiting the highest number of taxonomic orders across all area sizes. Notably, at very small forest areas, plantation initially exhibited greater biodiversity than pollard forests. However, from 100 m^2 onward, this trend reversed, with the pollard forest surpassing the plantation in taxonomic diversity. This shift can be attributed to the steeper curves observed in wild-grown and pollard forest compared to the plantation, emphasizing their greater capacity to support biodiversity as forest area expands. Overall, our

results highlight that increasing forest size enhances both ecological value and wave attenuation potential, regardless of forest type.

3.5. Cost analysis for forest type selection based on ecosystem service provision

The economic feasibility of dike-forest combinations is multifaceted and complex, but our results give a good framework (eq3). Based on the specific forest widths required for effective wave attenuation—500 m for wild-grown and plantation forest, and 150 m for a pollard forest—we calculated the investment needed to buy the area (eq4) using the average agricultural land price in 2024, being 83,900 € per hectare (Kadaster en Wageningen Economic Research, 2024). Forest establishment costs for willow planation and pollard forest (10,000 and 17,500 €/ha, respectively) were taken from De Vries and Dekker (2009) and adjusted for annual inflation (2–3 %) to reflect 2025 price levels. We used a conservative upper estimate of 10,000 € per hectare for the construction of the wild-grown forest, based on ranges of 3100–10,500 € per hectare (Di Fulvio and Lessa, 2025). Additionally, maintenance costs (eq5) were considered, with plantation and pollard forests requiring intensive coppicing every three years at 15000€ per hectare per coppicing run for manual coppicing (OBN Natuurkennis, 2025), while wild-grown forests have minor annual maintenance costs of 270 € per hectare (Teeuwen et al., 2020). The plantation of our study case was initially planned to be coppiced by machine, but the tree rows were planted too narrow, resulting in the need for coppicing manually. We obtained estimated total costs of €16.7 million for the plantation, €5.2 million for the pollard and €5.4 million wild-grown forest (Table 2, calculations see also Appendix D). To place these costs in context, we compared them with traditional dike reinforcement costs, which, without a hybrid nature-based solution, costs around €10 million per kilometer on average, based on estimates from the Dutch Flood Protection Program (Tromp et al., 2022). These are the costs to improve the existing dikes by e.g. heightening them with 1 m, and are thus not the costs to build an entire new dike. Average annual maintenance costs for dikes are estimated at around €11,500 per kilometer, covering regular inspections, vegetation management, and minor repairs (Brolsma, 2020). The total estimated costs for a traditional dike could be saved if another intervention type, i.e. a forest system is applied.

4. Discussion

This study explored whether there is a trade-off between biodiversity, wave attenuation, and economic feasibility in three willow forest types used as nature-based flood defenses. The results show that the wild-grown forest provided the highest ecological value, the pollard forest was most effective in wave attenuation, and the plantation forest offered a structured, predictable alternative. For the trade off, we set the three most important criteria to consider as space required, ecological value and costs and compared it (Fig. 10).

When integrating such nature-based systems into flood protection strategies, it is essential to evaluate ecological, safety and financial aspects. By presenting this case study, we offer a framework that can be adapted to other ecosystems, such as saltmarshes, supporting the development of hybrid solutions that integrate natural and engineered flood defenses. The fundamental aspects in case studies, namely required space, ecological value and costs can lead to well informed decisions. It can inspire the development of solutions that when adapted allow a better balance of multiple ecosystem services in a changing climate with competing interests and limited space.

4.1. Biodiversity considerations

4.1.1. Invertebrate diversity as an indicator of ecological value

Invertebrates play a direct role in ecosystem function, resilience, food web structure, species interactions (Cardoso et al., 2020), nutrient cycling (Yang and Gratton, 2014) and pollination (Ollerton et al., 2011) and invertebrate species richness and abundance often correlate with overall biodiversity making them reliable indicators (Landmann et al., 2023). Long-term monitoring of invertebrate populations provides valuable data on biodiversity trends and the impacts of conservation efforts (Hallmann et al., 2017).

We used ground-dwelling invertebrates as a proxy for biodiversity, recognizing their fundamental role at the base of the food web (Lister and Garcia, 2018). Our results indicate that wild-grown forests provide the most favorable conditions for invertebrate diversity, supported by their extensive litter layer and greater structural heterogeneity. Sampling only ground-dwelling invertebrates potentially underestimated the biodiversity of pollarded and wild-grown forests, which also host tree-dwelling invertebrates in the canopy, stems, and hollows. Given that tree hollows in pollard forests also provide critical habitats for saproxylic insects (Henneberg et al., 2021; Sebek et al., 2013), incorporating flying and tree-dwelling insects would allow to capture the full ecological complexity of the different forest types and multi-taxa or canopy-based surveys are highly recommended for future studies. Also, using invertebrate order richness as a proxy, rather than conducting a comprehensive assessment is a significant simplification and this needs to be elaborated in future studies.

Invertebrate body size was determined for beetles and spiders, as it serves as a bioindicator of habitat quality, resilience, and ecosystem function (Kalinkat et al., 2015). We found the largest range in the wild-grown forest as well as larger specimen. A diverse range of invertebrate sizes and particularly larger-bodied species indicates higher structural complexity, abundant resources, and greater resistance to environmental stressors (Kalinkat et al., 2015; Whitman, 2008). Hence, their presence is an indicator of stable, mature ecological conditions. Body size is a pivotal trait influenced by multiple environmental and biological factors, including nutrition, temperature, competition, and predation, which in turn shape key functional attributes such as feeding ability, locomotion, defense, and reproductive success, as clearly shown for Orthoptera (Whitman, 2008). Acting as a central ecological converter, body size generates complex feedback loops that impact fitness

Table 2
Estimated 50-year costs for dike-forest combinations and traditional dike reinforcement, including land, maintenance, and reinforcement expenses, the construction costs of a forest but not taking into account any dike construction nor any reinforcement cost of an existing dike when a forest is constructed in front. [x]calculated using the 3-yearly coppicing costs [1]Includes one-time dike reinforcement cost of €10.6 million.

Intervention Type	Required Width (m)	Area size (ha)	Land Price (€/ha)	Forest construction costs (€/ha)	Maintenance Type	Maintenance Cost annual (€/ha for forests; €/km for dike)	Coppicing costs over 50 years[x] (€M)	Estimated Cost – over 50 years (€M)
Wild-grown forest	500	50	83,900	10,000	Minor maintenance	270	N/A	5.4
Plantation	500	50	83,900	10,000	Manual coppicing	N/A	12	16.7
Pollard forest	150	15	83,900	17,500	Manual coppicing	N/A	3.6	5.2
Traditional Dike	N/A	N/A	N/A	N/A	Regular inspection & minor repairs	11.500	N/A	10.6[1]

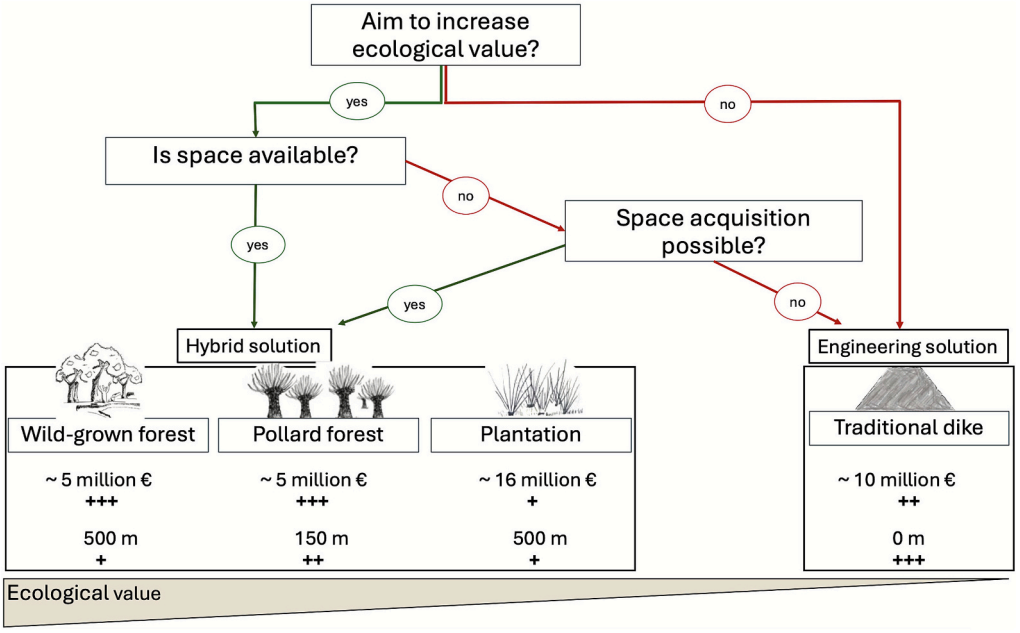


Fig. 10. Decision tree in which the trade off with three most important elements to consider and scores of the flood defense solutions with costs and required space and gradient of ecological value. The more crosses, the better.

and resource acquisition, making it a crucial yet intricate aspect of ecological research. In this context, the presence of a wide body-size distribution and especially larger individuals reflects not only habitat complexity but also higher resistance to environmental stressors (Kalinkat et al., 2015). Our findings show that in the wild-grown forest, spiders and beetles reached the largest sizes, and the overall insect community exhibited a broader size distribution, with most size categories represented. Larger-bodied invertebrates typically indicate high-quality habitats, as they require abundant resources, develop more slowly and are sensitive to disturbance, and often occupy higher trophic levels within a well-functioning food web. In contrast, size distribution in plantation and pollard forest was less uniform, and measured invertebrates were smaller, reinforcing the higher ecological value of the wild-grown forest compared to the other two forest types.

4.1.2. *Structural heterogeneity as a driver of biodiversity differences*

Forest structure plays a key role in shaping biodiversity by providing a variety of microhabitats. The wild-grown forest exhibited the highest structural heterogeneity, with trees at various growth stages, an observed more dynamic understory, and fallen trees creating diverse niches. This aligns with previous findings from the Biesbosch where natural succession in unmanaged willow forests led to higher plant species diversity and the formation of distinct biotopes (Bijlsma et al., 2009). Forest structural heterogeneity is closely linked to biodiversity. Among the studied sites, the wild-grown forest consistently exhibited the greatest structural complexity, as shown by remote sensing and in situ measurements.

Our findings serve as a relative comparison among the three forests rather than a comprehensive evaluation of structural heterogeneity. The wild-grown forest was expected to show greater heterogeneity, as both the pollard forest and the plantation represent managed systems with more uniform structures. This variation was also reflected in the biological data, with higher litter accumulation and significantly distinct and greater invertebrate alpha diversity in the wild-grown forest. Overall, these findings are consistent with previous research showing that structural complexity offers a diversity of microhabitats that support species richness (Heidrich et al., 2023). Hekkala et al. (2023) show that a habitat heterogeneity score is the strongest predictor of the number and abundance of red-listed species in boreal coniferous forests. Even partial measurements of heterogeneity can provide ecologically meaningful insight, especially when combined with biodiversity observations. In temperate forests in Central Europe, forest stand heterogeneity positively influences ecological diversity and redundancy across multiple animal taxa (Heidrich et al., 2023). However, heterogeneity-diversity effects can vary, with both positive and negative responses observed, showing the complexity in heterogeneity–diversity relationships (Heidrich et al., 2020).

While the pollard forest did not exhibit structural heterogeneity in our measurements, pollarded trees are known to provide unique microhabitats, particularly through the frequent development of tree hollows. Although we did not quantify this, we observed many tree hollows during fieldwork, suggesting an additional layer of habitat complexity. Pollarded trees have a substantially higher probability of developing hollows compared to non-pollarded trees. For instance, in willows with a DBH of 50 cm, approximately 75 % of pollarded trees had hollows, compared to only about 30 % of non-pollarded trees (Sebek et al., 2013). These tree hollows are crucial in supporting biodiversity, offering stable temperature and humidity conditions essential for the survival of saproxylic insects, species that depend on decaying wood trees (Henneberg et al., 2021; Sebek et al., 2013). A study on saproxylic beetles in German forests found that tree hollow characteristics, such as entrance size and the number of surrounding microhabitat structures, significantly influence beetle diversity (Henneberg et al., 2021). It would be of great value to quantify the tree hollows in a pollard forest system and compare this to other forest types. However, despite their high prevalence of tree hollows, pollard forests lack significant amounts of deadwood on the ground and fallen trees. But dead trees have a critical role for biodiversity (Hekkala et al., 2023) and have been shown to positively correlate with species richness of saproxylic beetles (Henneberg et al., 2021). The overall more homogeneous canopy and ground structure may limit biodiversity potential compared to wild-grown systems.

4.2. *Refining wave models via forest structure*

The wave model showed that regardless the tree shape in the forest, the wider a forest, the greater the wave attenuation. That a wider forest attenuates waves more than smaller forests was also found for mangrove forests, although with uncertainties below 500 m width and dependent

on local conditions (van Wesenbeeck et al., 2025). Given that the tree frontal area is a crucial component in flood safety (Kalloe et al., 2022), future studies should focus on estimating accurately the tree frontal area of a forest of interest, which could be achieved using terrestrial laser scanners (TLS) in the field (Arseniou et al., 2021; Calders et al., 2020). The method to use TLS is presented by Dunlop et al. (2025), who quantified mangrove attributes using TLS. Scanning during winter, when trees are leafless, would provide precise models of stems and branches, avoiding obstructions caused by leaves in spring or summer.

In addition to specifying stems and branches of living trees, the presence of dead standing and fallen trees can further affect the tree frontal area and roughness of the vegetation layer. Although not explicitly included in our model, dead trees may contribute substantially to near-ground biomass distribution and flow obstruction. Future research should explicitly quantify and include standing and fallen dead trees in wave attenuation models.

Field assessments and wave modelling studies could include other vegetation types in the forest. In our case study we used willow species and accordingly drag coefficients (Cd) in the simulations (Fig. 3) were derived for 6-m tall, pollarded willows by van Wesenbeeck et al. (2022), but could differ for other tree shapes. Therefore, each case needs to evaluate these variations in drag coefficients to refine models and improve accuracy, similar to the approach taken by Kalloe et al. (2022), who demonstrated that drag coefficients for woody vegetation can vary substantially (from 0.94 to 1.70) depending on how vegetation structure is measured and represented. Future research should specifically investigate how leaf presence and structural heterogeneity within the forest influence drag coefficients. Also, improved models, such as e.g. presented by Hu et al. (2025) allow to further refine the method to predict wave attenuation, by making the complications of the varying drag coefficient obsolete.

Beyond spatial variation in drag, temporal changes associated with coppice regrowth also influence wave attenuation capacity. The timing of storm events relative to coppice cycles can affect wave reduction in managed willow forests. Immediately after coppicing, reduced branch length and canopy density lower resistance to wave energy, whereas attenuation increases as regrowth progresses. Our in situ study, conducted 2.5 years after coppicing (November–December 2020), provided the data used to parameterize the model and therefore represents an intermediate stage of regrowth. To maintain consistent protection, coppicing could be staggered across forest sections so that some areas retain mature vegetation with higher wave reduction capacity.

4.3. Integrating cost and benefit considerations: a key element for future feasibility studies

Nature-based solutions are increasingly promoted for their multifunctionality (Alves et al., 2024). Their large-scale adoption depends primarily on demonstrating the functionality and economic feasibility in terms of ecosystem-services provided to enhance climate resilience, and only secondary on ecological value (van Zanten et al., 2023). Trade-off evaluations may help address this gap by enabling comparison of alternatives, and estimation of the cost-efficiency of hybrid dike-forest systems relative to traditional infrastructure. This is particularly relevant in densely populated deltas, where space, budget constraints, and sustained protective performance are critical factors.

The cost analysis presented here focused on the reinforcement of existing dikes and the establishment of a forest in front of existing dikes in need for maintenance. We assume in this calculation that constructing a willow forest in front of the dike sufficiently attenuates wave energy so that no further dike reinforcement is required, neither hard nor soft (e.g. renewed grass cover). Comparable hybrid, nature-based solutions have proven cost-effective; for example, Vuik et al. (2019) reported that 1 m of dike heightening costs €5.4–14.9 million, whereas the establishment of a 300 m-wide salt-marsh foreshore with a 100 m-wide high-marsh zone costs only €1.5–3.9 million. Although calculations typically are site-specific, such examples highlight the potential economic advantage of hybrid dike-forest systems, warranting detailed cost-effectiveness assessments in future studies. Hence we recommend to always perform a site specific cost-effectiveness assessment before deciding on applying willow-forest hybrid solutions or not in future flood defense works.

While simple in concept, incorporating a basic cost calculation is a crucial step towards assessing the feasibility and optimization potential of dike-forest systems. Such analysis opens the discussion on how realistic and scalable these nature-based solutions truly are. From this starting point, cost assessments expand in complexity, ranging from the price of forest or plantation establishment (e.g. purchasing and planting different tree species) (see e.g. Teeuwen et al., 2020; Di Fulvio and Lessa, 2025), to the specific structural requirements of a given dike, which can vary widely in costs. For example, dike reinforcement costs have shown considerable variation in recent Dutch projects: the Houtribdijk was reinforced at approximately €3.6 million per kilometer, while the Prins Hendrik Sand Dike and the Hondsbossche Dunes reached €18.3 million and €26.3 million per kilometer, respectively (Oerlemans et al., 2021).

Other cost factors include varying land acquisition, periodic replanting, and the lifespan of intensively managed willow stands, which may be shorter under coppicing regimes (Sebek et al., 2013). In addition, future economic evaluations should integrate government tools (e.g. in the Netherlands from Rijkswaterstaat), account for market demand for biomass, materials, and especially the value of ecosystem services. These services include carbon sequestration, improved habitat quality and increased biodiversity, including pollinators critical to agriculture. However, while these ecological benefits are often acknowledged, their monetary value remains poorly quantified.

Ecosystem services were not monetized in this study, although their inclusion could substantially affect the cost–benefit balance. Brander et al. (2024) demonstrated that economic values of ecosystem services vary greatly across and within biomes, highlighting the complexity of their valuation. The valuation and mapping of ecosystem services are inherently interdisciplinary, requiring the integration of specific ecological and economic approaches to capture all biophysical and socio-economic dimensions (Schägner et al., 2013). In our study we considered purely the cost of implementation and simple maintenance while all the potential ecological benefits were not monetized. Future assessments should therefore always weigh side by side both the ecological and economic approaches, as unaccounted ecosystem benefits may significantly influence the overall value of forest and hybrid dike systems.

For example carbon sequestration: Willow plantations, when managed as short-rotation coppice (SRC), have been shown to act as carbon sinks, with a significant increase in carbon stocks for full carbon budgets (0.15–0.45 Mg C per ha per yr) (Rytter et al., 2015) or the aboveground biomass (6.78 Mg C per ha per yr) (Riccioli et al., 2020). SRC willows enhanced soil organic carbon concentrations by almost 1 % over a 12-year period (11.66 Mg C per ha per yr) for a total gross carbon stock (Schrama et al., 2016). There is thus a meaningful contribution of willows in carbon sequestration and revenues that should be considered in holistic cost-benefit analyses.

Willow branches were historically used in hydraulic engineering and have regained attention as bio-based building material (Van Aalsburg, 2021). Pilot initiatives, like a “Willows in Business” project funded by the Province of South Holland, demonstrate the broader economic and multifunctional potential of willow cultivation in climate-adaptive land use. By developing local production chains for willow-based construction materials, alternative income models are created for farmers, while the willow plantations act for carbon reduction, flood protection, and the mitigation of soil subsidence (Provincie Zuid-Holland, 2025). Willow shoots are being explored as low-impact foundation material for temporary housing, bike paths, and wetland infrastructure, demonstrating both ecological compatibility and social relevance (Veenweiden Innovatiecentrum, 2025).

4.4. Outlook and opportunities

In our study we present a valuable approach, applicable to practical cases in complex settings. The applied method allowed us to develop a clear decision tree to support managers (Fig. 10) and highlight key aspects for consideration in each case. While the framework offers a strong starting point, it should be further refined when applied to specific real-world cases. The latter would require site-specific biodiversity measurements extending over more ecological classes than we looked at, and case specific modelling accounting for specific factors such as local tree dimensions and local hydraulic conditions. Having such local parameters would enhance the applicability of the presented approach much further and allow for tailoring to local contexts and specific management objectives.

The principles underlying our approach could potentially be applied globally, particularly in regions with similar ecological, hydrological, or land-use conditions. Low-lying floodplains, deltas, and riparian zones occur worldwide. For example, the Mississippi Alluvial Valley with a lower flood plain and delta of 11 million ha, where it supports extensive willow stands (Gardiner and Stanturf, 2014). We recommend that future studies explore the spatial extent of areas where nature-based solution with different types of willow forests can be applied.

It is noted that presented results highlight the ecological value of wild-grown, structurally diverse forest systems and suggest prioritizing mosaic of forest structures at multiple spatial scales, like shown in Uhl et al. (2024), as a key ecological asset when optimizing nature-based flood defenses for biodiversity. We should however acknowledge that heterogeneity will (relative to homogeneous structured forests) always translate into a higher space demand to achieve the wave-attenuation required for flood safety. The spatial requirement of approximately 500 m can be a key practical limitation for application of the wild-grown forest compared to the pollard forest in densely populated deltas, where land availability is strongly restricted. If land acquisition is possible but limited, the pollard forest offers higher spatial efficiency, making it a more feasible choice in areas with limited space.

The high diversity value of the wild-grown forest poses a critical challenge on the management of willow forests, especially those found harboring unique and endangered flood forest species. Many wild-grown willow stands in the Netherlands are currently collapsing as the trees reach the end of their lifespan. Natural recruitment of willows in abandoned willow cultivation stands has proven to be limited (Bijlsma et al., 2009) due to the thick understory. The latter makes it increasingly difficult to maintain, so let alone expand willow flood forests on the long run, despite being a legal requirement by the European Water Framework Directive (WFD). Additionally, many of these willow flood forests fall within Natura 2000 areas, where their restoration and maintenance contribute to achieving European conservation objectives under the Habitats and Birds Directives. Combining the WFD-goal with cultural heritage goals, old-growth willow stands are being converted back into pollard willow stands. Although this would lower biodiversity values as put forwards by the current paper, it does secure the persistence of the willow forest on the long run. An alternative route would be to manage understory growth to help young willow-trees establish and to stimulate the development of a more diverse tree community with species that are adapted to establish in mature forest stands and can survive in the tidal or floodplain conditions. Historically, the dominant species in the study region was *Alnus glutinosa* (Pierik et al., 2023), a species that does not, like many *Salix* species, depend on disturbance to establish. Moreover, it has been suggested in a study by Saccon et al. (2025) that *Alnus* is better to resist both flooding and salt stress, both typically stressors in estuarine conditions. A crucial concern across all willow-forest types is the limited tree species diversity, particularly in formerly planted areas (Bijlsma et al., 2009). Genetic diversity enhances ecosystem resilience (Perrow and Davy, 2002), yet traditional planting methods often rely on clonal material, which may reduce long-term adaptability. Hence, to preserve wild-grown forests as nature-based solutions for improved flooding safety, stimulating tree biodiversity might be an essential management avenue.

Future feasibility studies should take an integrated approach, that accounts not only for physical and financial parameters, but also for the full range of ecosystem services of the different forest types. This should also include those ecosystem services that cannot easily be quantified in euros, but obviously do have significant (economic) value, such as e.g. biodiversity. Moreover, it should be considered to broaden the view and i) look at the tree biodiversity as an essential strategy to enhance biodiversity and resilience of the system and ii) look at the long-term management practice to guarantee safety also if it may require active interventions.

5. Conclusion: finding the right balance

Our findings show that no single nature-based flood defense design is universally superior. Instead, the optimal design is site-specific. For example, the wild-grown forest in our case study delivered similar wave attenuation as the plantation forest, but at lower cost and with higher ecological benefit. In contrast, the pollard forest achieved strong wave reduction in a more compact area, though with higher maintenance demands and at lower biodiversity. These examples highlight the importance of tailoring strategies to the local context, carefully weighing spatial, ecological, economic, and social factors.

The optimal design of dike-forest systems is inherently context-dependent, shaped by the dominant ecosystem service priorities and constraints of each location. A financially viable system can simultaneously enhance ecological value, strengthen ecosystem resilience, and provide effective flood protection. However, to ensure substantial ecological value whether enhancing an existing forest or creating a new one, a certain degree of structural and compositional heterogeneity should be incorporated. Looking ahead, integrating remote sensing within situ biodiversity assessments could offer a powerful tool for long-term monitoring of habitat development and ecological outcomes. Such insights will be critical for refining and cost-effective upscaling of nature-based flood defense strategies and ensuring their effectiveness under changing climate conditions.

CRediT authorship contribution statement

Corinne van Starrenburg: Writing – review & editing, Writing – original draft, Visualization, Validation, Software, Methodology, Investigation, Formal analysis, Data curation, Conceptualization. **Alejandra Gijón Mancheño:** Writing – review & editing, Writing – original draft, Visualization, Validation, Software, Methodology, Investigation, Formal analysis. **Johan van de Koppel:** Writing – review & editing, Supervision, Funding acquisition, Conceptualization. **Daphne van der Wal:** Writing – review & editing, Supervision, Methodology, Funding acquisition, Conceptualization. **Matthijs H. Slegt:** Investigation. **Maarten J.J. Schrama:** Writing – review & editing, Validation, Methodology. **Matty P. Berg:** Writing – review & editing, Validation, Methodology. **Bregje K. van Wesenbeeck:** Writing – review & editing, Funding acquisition, Conceptualization. **Su A. Kalloe:** Writing – review & editing, Software, Methodology. **Bas Hofland:** Writing – review & editing, Validation, Funding acquisition. **Tjeerd J. Bouma:** Writing – review & editing, Validation, Supervision, Project administration, Methodology, Funding acquisition, Conceptualization.

Declaration of competing interest

The authors declare the following financial interests/personal relationships which may be considered as potential competing interests: (Corinne van Starrenburg reports financial support was provided by Dutch Research Council. If there are other authors, they declare that they have no known competing financial interests or personal relationships that could have appeared to influence the work reported in

this paper.)

Appendix A. Supplementary data

Supplementary data to this article can be found online at https://doi.org/10.1016/j.ecoleng.2025.107886.

Data availability

Data will be made available on request.

References

Alves, A., van Opstal, C., Keijzer, N., Sutton, N., Chen, W.S., 2024. Planning the multifunctionality of nature-based solutions in urban spaces. Cities 146. https://doi.org/10.1016/j.cities.2023.104751.

Arseniou, G., Macfarlane, D.W., Seidel, D., 2021. Woody surface area measurements with terrestrial laser scanning relate to the anatomical and structural complexity of urban trees. Remote Sens. 13 (16). https://doi.org/10.3390/rs13163153.

Aylott, M.J., Casella, E., Tubby, I., Street, N.R., Smith, P., Taylor, G., 2008. Yield and spatial supply of bioenergy poplar and willow short-rotation coppice in the UK. New Phytol. 178, 358–370. https://doi.org/10.1111/j.1469-8137.2008.02396.x.

Bao, T.Q., 2011. Effect of mangrove forest structures on wave attenuation in coastal Vietnam. Oceanologia 53 (3), 807–818. https://doi.org/10.5697/oc.53-3.807.

Barendregt, A., Swarth, C.W., 2013. Tidal freshwater wetlands: variation and changes. Estuar. Coasts 36 (3), 445–456. https://doi.org/10.1007/s12237-013-9626-z.

Beselly, S.M., Grueters, U., van Der Wegen, M., Reyns, J., Dijkstra, J., Roelvink, D., 2023. Modelling mangrove-mudflat dynamics with a coupled individual-based-hydro-morphodynamic model. Environ. Model. Softw. 169. https://doi.org/10.1016/j.envsoft.2023.105814.

Bijlsma, R.J., Weeda, E., Verkaik, E., met medewerking van C. Huibers, W.H. van Orden, G. M. van R. & A. T. F. H, 2009. Wentelwilgen, wortelkluiten en wave dieback. Diversiteit door natuurlijke processen in bosreservaten in de Biesbosch.

Brander, L.M., de Groot, R., Schägner, J.P., Guisado-Goñi, V., van 't Hoff, V., Solomonides, S., McVittie, A., Eppink, F., Sposato, M., Do, L., Ghermandi, A., Sinclair, M., Thomas, R., 2024. Economic values for ecosystem services: a global synthesis and way forward. Ecosyst. Serv. 66. https://doi.org/10.1016/j.ecoser.2024.101606.

Brolsma, R., 2020. Coastal wiki: Tabellen aanleg- en beheerkosten.

Calders, K., Adams, J., Armston, J., Bartholomeus, H., Bauwens, S., Bentley, L.P., Chave, J., Danson, F.M., Demol, M., Disney, M., Gaulton, R., Krishna Moorthy, S.M., Levick, S.R., Saarinen, N., Schaaf, C., Stovall, A., Terryn, L., Wilkes, P., Verbeeck, H., 2020. Terrestrial laser scanning in forest ecology: Expanding the horizon. In: Remote Sensing of Environment, vol. 251. Elsevier Inc. https://doi.org/10.1016/j.rse.2020.112102

Cardoso, P., Barton, P.S., Birkhofer, K., Chichorro, F., Deacon, C., Fartmann, T., Fukushima, C.S., Gaigher, R., Habel, J.C., Hallmann, C.A., Hill, M.J., Hochkirch, A., Kwak, M.L., Mammola, S., Ari Noriega, J., Orfinger, A.B., Pedraza, F., Pryke, J.S., Roque, F.O., Samways, M.J., 2020. Scientists' warning to humanity on insect extinctions. In: Biological Conservation, vol. 242. Elsevier Ltd. https://doi.org/10.1016/j.biocon.2020.108426

De Vries, M.B., Dekker, F., 2009. Ontwerp groene golfremmende dijk Fort Steurgat bij Werkendam. Deltares.

Department for Environment, Food and Rural Affairs (DEFRA), 2004. Best Practice Guidelines for Short Rotation Coppice. London, United Kingdom.

Di Fulvio, F., Lessa, A., 2025. D4.4 Report on EU Forest Management Costing Module and Green Jobs Calculator (ForestNavigator: Navigating European Forests and Forest Bioeconomy Sustainability to EU Climate Neutrality). retrieved from: https://www.forestnavigator.eu/wp-content/uploads/FN_D4.4-ForestManagement-costing.pdf.

Duits, 2020. Hydra-NL – Gebruikershandleiding – Versie 2.8 [HKV-rapport PR4315.10]. Matthijs Duits. HKV lijn in water, oktober 2020.

Dunlop, T., Mancheño, A.G., Glamore, W., Felder, S., van Wesenbeeck, B.K., 2025. Quantifying mangrove forest attributes using terrestrial laser scanning. Estuar. Coasts 48 (4). https://doi.org/10.1007/s12237-025-01533-0.

Ehbrecht, M., Seidel, D., Annighöfer, P., Kreft, H., Köhler, M., Zemp, D.C., Puettmann, K., Nilus, R., Babweteera, F., Willim, K., Stiers, M., Soto, D., Boehmer, H.J., Fisichelli, N., Burnett, M., Juday, G., Stephens, S.L., Ammer, C., 2021. Global patterns and climatic controls of forest structural complexity. Nat. Commun. 12 (1). https://doi.org/10.1038/s41467-020-20767-z.

European Commission, 2011. Strategy to 2020. https://doi.org/10.2779/24101.

Fang, Z.-F., Zhao, S.-D., Skvortsov, A.K., 1999. Salicaceae. In: Wu, Z.-Y., Raven, P.H. (Eds.), Flora of China, Vol. 4. Science Press, Beijing, China, pp. 162–274. St. Louis, MO: Missouri Botanical Garden Press.

Franklin, J.F., Spies, T.A., Van Pelt, R., Carey, A.B., Thornburgh, D.A., Berg, D.R., Lindenmayer, D.B., Harmon, M.E., Keeton, W.S., Shaw, D.C., Bible, K., Chen, J., 2002. Disturbances and structural development of natural forest ecosystems with silvicultural implications, using Douglas-fir forests as an example. For. Ecol. Manag. 155 (1–3), 399–423. https://doi.org/10.1016/S0378-1127(01)00575-8.

Gardiner, E.S., Stanturf, J.A., 2014. Use of poplar and willow to create forested riparian buffers in the Lower Mississippi Alluvial Valley. In: Isebrands, J.G., Richardson, J. (Eds.), Poplars and willows: Trees for society and the environment. CABI, Boston, MA, pp. 258–272. https://doi.org/10.1079/9781780641089.0258. Rome, Italy: FAO.

Gijón Mancheño, A., Jansen, W., Uijttewaal, W.S.J., Reniers, A.J.H.M., van Rooijen, A.A., Suzuki, T., Etminan, V., Winterwerp, J.C., 2021. Wave transmission and drag coefficients through dense cylinder arrays: implications for designing structures for mangrove restoration. Ecol. Eng. 165. https://doi.org/10.1016/j.ecoleng.2021.106231.

Gijón Mancheño, A., Vuik, V., van Wesenbeeck, B.K., Jonkman, S.N., van Hespen, R., Moll, J.R., Kazi, S., Urrutia, I., van Ledden, M., 2024. Integrating mangrove growth and failure in coastal flood protection designs. Sci. Rep. 14 (1). https://doi.org/10.1038/s41598-024-58705-4.

Gijsman, R., Horstman, E.M., van der Wal, D., Friess, D.A., Swales, A., Wijnberg, K.M., 2021. Nature-based engineering: a review on reducing coastal flood risk with mangroves. Front. Mar. Sci. 8 (July). https://doi.org/10.3389/fmars.2021.702412.

Gijsman, R., Horstman, E.M., Swales, A., MacDonald, I.T., Bouma, T.J., van der Wal, D., Wijnberg, K.M., 2024. Mangrove forest drag and bed stabilisation effects on intertidal flat morphology. Earth Surf. Process. Landf. 49 (3), 1117–1134. https://doi.org/10.1002/esp.5758.

Graham, J.M.R., 1980. The forces on sharp-edged cylinders in oscillatory flow at low keulegan-carpenter numbers. J. Fluid Mech. 97 (1), 331–346. https://doi.org/10.1017/S0022112080002595.

Gumbel, E.J., 1941. The return period of flood flows. Ann. Math. Stat. 12, 163–190. https://doi.org/10.1214/aoms/1177731747.

Hallmann, C.A., Sorg, M., Jongejans, E., Siepel, H., Hofland, N., Schwan, H., Stenmans, W., Müller, A., Sumser, H., Hörren, T., Goulson, D., De Kroon, H., 2017. More than 75 percent decline over 27 years in total flying insect biomass in protected areas. PLoS One 12 (10). https://doi.org/10.1371/journal.pone.0185809.

Hashim, A.M., Catherine, S.M.P., Takaijudin, H., 2013. Effectiveness of mangrove forests in surface wave attenuation: A review. In. Res. J. Appl. Sci. Eng. Technol. 5 (18), 4483–4488. Maxwell Science Publications. 10.19026/rjaset.5.4361.

Heidrich, L., Bae, S., Levick, S., Seibold, S., Weisser, W., Krzystek, P., Magdon, P., Nauss, T., Schall, P., Serebryanyk, A., Wöllauer, S., Ammer, C., Bässler, C., Doerfler, I., Fischer, M., Gossner, M.M., Heurich, M., Hothorn, T., Jung, K., Kreft, H., Schulze, E.-D., Simons, N., Thorn, S., Müller, J., 2020. Heterogeneity–diversity relationships differ between and within trophic levels in temperate forests. Nat. Ecol. Evol. 4 (9), 1204–1212. https://doi.org/10.1038/s41559-020-1245-z.

Heidrich, L., Brandl, R., Ammer, C., Bae, S., Bässler, C., Doerfler, I., Fischer, M., Gossner, M.M., Heurich, M., Heibl, C., Jung, K., Krzystek, P., Levick, S., Magdon, P., Schall, P., Schulze, E.D., Seibold, S., Simons, N.K., Thorn, S., Weisser, W.W., Wöllauer, S., Müller, J., 2023. Effects of heterogeneity on the ecological diversity and redundancy of forest fauna. Basic Appl. Ecol. 73, 72–79. https://doi.org/10.1016/j.baae.2023.10.005.

Hekkala, A.M., Jönsson, M., Kärvemo, S., Strengbom, J., Sjögren, J., 2023. Habitat heterogeneity is a good predictor of boreal forest biodiversity. Ecol. Indic. 148. https://doi.org/10.1016/j.ecolind.2023.110069.

Henneberg, B., Bauer, S., Birkenbach, M., Mertl, V., Steinbauer, M.J., Feldhaar, H., Obermaier, E., 2021. Influence of tree hollow characteristics and forest structure on saproxylic beetle diversity in tree hollows in managed forests in a regional comparison. Ecol. Evol. 11 (24), 17973–17999. https://doi.org/10.1002/ece3.8393.

Hu, Z., Temmerman, S., Zhu, Q., Wang, X., Wu, J., Xu, T., Schoutens, K., Suzuki, T., Yang, Z., Bouma, T.J., 2025. Predicting nature-based coastal protection by mangroves under extreme waves. Proc. Natl. Acad. Sci. USA 122 (12), e2410883122. https://doi.org/10.1073/pnas.2410883122.

International Federation of Red Cross and Red Crescent Societies (IFRC), 2012. Mangrove Plantation in Viet Nam: Measuring Impact and Cost Benefit [Case Study]. IFRC. https://www.ifrc.org/Global/Publications/disasters/reducing_risks/Case-study-Vietnam.pdf.

Kadaster, Wageningen Economic Research, 2024. https://asrrealestate.nl/huren-en-erfpachten/landelijk-vastgoed/grondprijzen/landelijk-overzicht.

Kalinkat, G., Jochum, M., Brose, U., Dell, A.I., 2015. Body size and the behavioral ecology of insects: Linking individuals to ecological communities. In: Current Opinion in Insect Science, vol. 9. Elsevier Inc., pp. 24–30. https://doi.org/10.1016/j.cois.2015.04.017

Kalloe, S.A., 2025. Wave Damping through Woody Vegetation. TU Delft. https://doi.org/10.4233/uuid:9e4b00ed-d9a5-4d4d-a8df-48f16fb025bd.

Kalloe, S.A., Hofland, B., Antolínez, J.A.A., van Wesenbeeck, B.K., 2022. Quantifying frontal-surface area of woody vegetation: a crucial parameter for wave attenuation. Front. Mar. Sci. 9 (March), 1–18. https://doi.org/10.3389/fmars.2022.820846.

Landmann, T., Schmitt, M., Ekim, B., Villinger, J., Ashiono, F., Habel, J.C., Tonnang, H.E. Z., 2023. Insect diversity is a good indicator of biodiversity status in Africa. Commun. Earth Environ. 4 (1). https://doi.org/10.1038/s43247-023-00896-1.

Lister, B.C., Garcia, A., 2018. Climate-driven declines in arthropod abundance restructure a rainforest food web. Proc. Natl. Acad. Sci. USA 115 (44), E10397–E10406. https://doi.org/10.1073/pnas.1722477115.

Lugo, A.E., Snedaker, S.C., 1974. The ecology of mangroves. Annu. Rev. Ecol. Syst. 5, 39–64. https://doi.org/10.1146/annurev.es.05.110174.000351.

Magurran, A.E., 2005. Measuring Biological Diversity, 3rd ed. Blackwell Science Ltd.

Markus-Michalczyk, H., Hanelt, D., 2019. Willow species vary in elevational occurrence and morphological characteristics on the tidal freshwater section of the Elbe estuary. Ecohydrol. Hydrobiol. 19 (1), 14–23. https://doi.org/10.1016/j.ecohyd.2018.08.006.

Markus-Michalczyk, H., Michalczyk, M., 2023. Floodplain forest restoration as a Nature-based solution to create climate-resilient communities in european lowland estuaries. Water 15 (3), 440. https://doi.org/10.3390/w15030440.

Mazda, Y., Magi, M., Ikeda, Y., Kurokawa, T., Asano, T., 2006. Wave reduction in a mangrove forest dominated by Sonneratia sp. Wetl. Ecol. Manag. 14 (4), 365–378. https://doi.org/10.1007/s11273-005-5388-0.

Mcgranahan, G., Balk, D., Mcgranahan, G., Bartlett, S., 2007. The rising tide : assessing the risks of climate change and human settlements in low elevation coastal zones, 19 (1), 17–37. https://doi.org/10.1177/0956247807076960.

Mendez, F.J., Losada, I.J., 2004. An empirical model to estimate the propagation of random breaking and nonbreaking waves over vegetation fields. Coast. Eng. 51 (2), 103–118. https://doi.org/10.1016/j.coastaleng.2003.11.003.

Menéndez, P., Losada, I.J., Torres-Ortega, S., Narayan, S., Beck, M.W., 2020. The global flood protection benefits of mangroves. Sci. Rep. 10 (1). https://doi.org/10.1038/s41598-020-61136-6.

Möller, I., Kudella, M., Rupprecht, F., Spencer, T., Paul, M., van Wesenbeeck, B.K., Wolters, G., Jensen, K., Bouma, T.J., Miranda-Lange, M., Schimmels, S., 2014. Wave attenuation over coastal salt marshes under storm surge conditions. Nat. Geosci. 7 (10), 727–731. https://doi.org/10.1038/ngeo2251.

OBN Natuurkennis, 2025. N17–05 Wilgengriend (n.d.). https://natuurkennis.nl/beheertypen/n17-cultuurhistorische-bossen/n17-05-wilgengriend/#onderwerp-1.

Oerlemans, C., Wegman, C., Jonkman, B., Aarninkhof, S., 2021. The impact and costs of Building with Nature projects. Terra et Aqua 165, 4–13. https://www.iadc-dredging.com/wp-content/uploads/2021/12/terra-et-aqua-165-4-spread.pdf.

Ollerton, J., Winfree, R., Tarrant, S., 2011. How many flowering plants are pollinated by animals? Oikos 120 (3), 321–326. https://doi.org/10.1111/j.1600-0706.2010.18644.x.

Perrow, M., Davy, A., 2002. In: Davy, A. (Ed.), Handbook of Ecological Restoration, Vol. 1. Cambridge University Press. https://doi.org/10.1017/CBO9780511549984.

Peters, B., Bijlsma, R.-J., Maas, G., 2021. Ooibossen, van Ooievaar tot Stroomlijn en verder.

Pierik, H.J., Moree, J.I.M., van der Werf, K.M., Roelofs, L., Albernaz, M.B., Wilbers, A., van der Valk, B., van Dinter, M., Hoek, W.Z., de Haas, T., Kleinhans, M.G., 2023. Vegetation and peat accumulation steer Holocene tidal–fluvial basin filling and overbank sedimentation along the Old Rhine River, The Netherlands. Sedimentology 70 (1), 179–213. https://doi.org/10.1111/sed.13038.

Pollen, N., Simon, A., Collison, A., 2013. Advances in assessing the mechanical and hydrologic effects of riparian vegetation on streambank stability. Riparian Vegetation and Fluvial Geomorphology 125–139. https://doi.org/10.1029/008WSA10.

Provincie Zuid-Holland. 2025 (n.d.). Kansen van de wilg als biogrondstof. Circulair Zuid-Holland. Retrieved March 27, 2025, from https://circulair.zuid-holland.nl/activiteit/kansen-van-de-wilg-als-biogrondstof/.

Riccioli, F., Nissim, W.G., Masi, M., Palm, E., Mancuso, S., Azzarello, E., 2020. Modelling the ecosystem services related to phytoextraction: carbon sequestration potential using willow and poplar. Appl. Sci. (Switz.) 10 (22), 1–18. https://doi.org/10.3390/app10228011.

Rijksdienst voor het Cultureel Erfgoed (RCE), 2025. Knotboom (cultuurhistorisch beheer) (n.d.).

Rotherham, I.D., 2022. Willows in the farming landscape: a forgotten eco-cultural icon. Biodivers. Conserv. 31 (10), 2495–2513. https://doi.org/10.1007/s10531-021-02324-2.

Rytter, R.M., Rytter, L., Högbom, L., 2015. Carbon sequestration in willow (Salix spp.) plantations on former arable land estimated by repeated field sampling and C budget calculation. Biomass Bioenergy 83, 483–492. https://doi.org/10.1016/j.biombioe.2015.10.009.

Saccon, E., van de Koppel, J., Bekhuis, W., Hulscher, S.J.M.H., Bouma, T.J., 2025. Historic human-induced species shift increases climate sensitivity of today's Western European floodplain forests: restoring past conditions for future resilience. Freshw. Biol. 70 (4). https://doi.org/10.1111/fwb.70034.

Saleh, F., Weinstein, M.P., 2016. The role of nature-based infrastructure (NBI) in coastal resiliency planning: a literature review. J. Environ. Manag. 183, 1088–1098. https://doi.org/10.1016/j.jenvman.2016.09.077.

Sanders, M.E., Henkens, R.J.H.G., Slijkerman, D.M.E., WUR, 2019. Convention on Biological Diversity - Sixth National Report of the Kingdom of the Netherlands. WOt-Technical Report 156.

Schägner, J.P., Brander, L., Maes, J., Hartje, V., 2013. Mapping ecosystem services' values: Current practice and future prospects. In: Ecosystem Services, Vol. 4, pp. 33–46. https://doi.org/10.1016/j.ecoser.2013.02.003.

Schepers, J.A.M., 1989. Een landelijk overzicht van de grienden. Nederlands Bosbouwtijdschrift 61 (3), 88–96.

Schoonees, T., Gijón Mancheño, A., Scheres, B., Bouma, T.J., Silva, R., Schlurmann, T., Schüttrumpf, H., 2019. Hard structures for coastal protection, towards greener designs. Estuar. Coasts 42 (7), 1709–1729. https://doi.org/10.1007/s12237-019-00551-z.

Schrama, M., Vandecasteele, B., Carvalho, S., Muylle, H., van der Putten, W.H., 2016. Effects of first- and second-generation bioenergy crops on soil processes and legacy effects on a subsequent crop. GCB Bioenergy 8, 136–147. https://doi.org/10.1111/gcbb.12236.

Sebek, P., Altman, J., Platek, M., Cizek, L., 2013. Is active management the key to the conservation of saproxylic biodiversity? Pollarding promotes the formation of tree hollows. PLoS One 8 (3), 1–6. https://doi.org/10.1371/journal.pone.0060456.

Stanton, B.J., Serapiglia, M.J., Smart, L.B., 2014. The domestication and conservation of Populus and Salix genetic resources. In: Isebrands, J.G., Richardson, J. (Eds.), Poplars and Willows: Trees for Society and the Environment. CABI, Boston, MA, pp. 258–272. https://doi.org/10.1079/9781780641089.0258. Rome, Italy: FAO.

Suzuki, T., Zijlema, M., Burger, B., Meijer, M.C., Narayan, S., 2012. Wave dissipation by vegetation with layer schematization in SWAN. Coast. Eng. 59 (1), 64–71. https://doi.org/10.1016/j.coastaleng.2011.07.006.

Swarth, C.W., Delgado, P., Whigham, D.F., 2013. Vegetation dynamics in a tidal freshwater wetland: a long-term study at differing scales. Estuar. Coasts 36 (3), 559–574. https://doi.org/10.1007/s12237-012-9568-x.

Teeuwen, S., Reichgelt, A., Oldenburger, J., 2020. Factsheets kostenindicatie aanleg bos & landschapselementen. Stichting Probos. https://gereedschapskistbosennatuur.nl/wp-content/uploads/2024/11/factsheets-kostenindicatie-aanleg-bos-landschapselementen-2020.pdf.

Temmerman, S., Meire, P., Bouma, T.J., Herman, P.M.J., Ysebaert, T., De Vriend, H.J., 2013. Ecosystem-based coastal defence in the face of global change. Nature 504 (7478), 79–83. https://doi.org/10.1038/nature12859.

Tews, J., Brose, U., Grimm, V., Tielbörger, K., Wichmann, M.C., Schwager, M., Jeltsch, F., 2004. Animal species diversity driven by habitat heterogeneity/diversity: The importance of keystone structures. In: Journal of Biogeography, Vol. 31, Issue 1. Blackwell Publishing Ltd, pp. 79–92. https://doi.org/10.1046/j.0305-0270.2003.00994.x.

Tromp, E., Te Nijenhuis, A., Knoeff, H., 2022. The Dutch flood protection programme: taking innovations to the next level. Water (Switzerland) 14 (9). https://doi.org/10.3390/w14091460.

Uhl, B., Schall, P., Bässler, C., 2024. Achieving structural heterogeneity and high multi-taxon biodiversity in managed forest ecosystems: A European review. In: Biodiversity and Conservation. Springer Science and Business Media B.V. https://doi.org/10.1007/s10531-024-02878-x.

Van Aalsburg, B.V., 2021. Wilgenhout: Duurzaam bouwmateriaal voor de waterbouw, 3. OTAR, pp. 28–29. https://www.otar.nl/wp-content/uploads/2021/06/OTAR-3-2021-Wilgenhout-duurzaam-bouwmateriaal-voor-de-waterbouw.pdf.

van Hespen, R., Hu, Z., Peng, Y., Borsje, B.W., Kleinhans, M., Ysebaert, T., Bouma, T.J., 2021. Analysis of coastal storm damage resistance in successional mangrove species. Limnol. Oceanogr. 66 (8), 3221–3236. https://doi.org/10.1002/lno.11875.

van Wesenbeeck, B.K., Mulder, J.P.M., Marchand, M., Reed, D.J., De Vries, M.B., De Vriend, H.J., Herman, P.M.J., 2014. Damming deltas: a practice of the past? Towards nature-based flood defenses. Estuar. Coast. Shelf Sci. 140, 1–6. https://doi.org/10.1016/j.ecss.2013.12.031.

van Wesenbeeck, B.K., Wolters, G., Antolínez, J.A.A., Kalloe, S.A., Hofland, B., de Boer, W.P., Çete, C., Bouma, T.J., 2022. Wave attenuation through forests under extreme conditions. Sci. Rep. 12 (1), 1–8. https://doi.org/10.1038/s41598-022-05753-3.

van Wesenbeeck, B.K., van Zelst, V.T.M., Antolinez, J.A.A., de Boer, W.P., 2025. Quantifying uncertainty in wave attenuation by mangroves to inform coastal green belt policies. Commun. Earth Environ. 6 (1). https://doi.org/10.1038/s43247-025-02178-4.

van Zanten, B., Gutierrez Goizueta, G., Brander, L., Gonzalez Reguero, B., Griffin, R., Kapur Macleod, K., Alves, A., Midgley, A., Diego Herrera, L., Jongman, B., 2023. Assessing the Benefits and Costs of Nature-Based Solutions for Climate Resilience: A Guideline for Project Developers Cover Design. www.worldbank.org.

Västilä, K., Järvelä, J., 2018. Characterizing natural riparian vegetation for modelling of flow and suspended sediment transport. J. Soils Sediments 18 (10), 3114–3130. https://doi.org/10.1007/s11368-017-1776-3.

Veenweiden Innovatiecentrum. 2025 (n.d.). Wilgen in Business. Retrieved March 27, 2025, from https://www.veenweiden.nl/activiteiten/wilgen-in-business/.

Vuik, V., Jonkman, S.N., Borsje, B.W., Suzuki, T., 2016. Nature-based flood protection: the efficiency of vegetated foreshores for reducing wave loads on coastal dikes. Coast. Eng. 116, 42–56. https://doi.org/10.1016/j.coastaleng.2016.06.001.

Vuik, V., Borsje, B.W., Willemsen, P.W.J.M., Jonkman, S.N., 2019. Salt marshes for flood risk reduction: quantifying long-term effectiveness and life-cycle costs. Ocean Coast. Manag. 171, 96–110.

Whitman, D.W., 2008. The significance of body size in the Orthoptera: a review. J. Orthop. Res. 17 (2), 117–134. https://doi.org/10.1665/1082-6467-17.2.117.

Yang, L.H., Gratton, C., 2014. Insects as drivers of ecosystem processes. Curr. Opin. Insect Sci. 2, 26–32. https://doi.org/10.1016/j.cois.2014.06.004.

Zhai, T., Wang, J., Fang, Y., Qin, Y., Huang, L., Chen, Y., 2019. Assessing ecological risks caused by human activities in rapid urbanization coastal areas: towards an integrated approach to determining key areas of terrestrial-oceanic ecosystems preservation and restoration. Sci. Total Environ. 708, 135153. https://doi.org/10.1016/j.scitotenv.2019.135153.

Zhou, X., Dai, Z., Carniello, L., Long, C., Wang, R., Luo, J., Huang, Z., 2022. Linkage between mangrove wetland dynamics and wave attenuation during a storm–a case study of the Nanliu Delta, China. Mar. Geol. 454. https://doi.org/10.1016/j.margeo.2022.106946.

Zhu, Z., Vuik, V., Visser, P.J., Soens, T., van Wesenbeeck, B., van de Koppel, J., Jonkman, S.N., Temmerman, S., Bouma, T.J., 2020. Historic storms and the hidden value of coastal wetlands for nature-based flood defence. Nat. Sustainability 3 (10), 853–862. https://doi.org/10.1038/s41893-020-0556-z.